Robust induced ℓ2−ℓ∞ optimal control of discrete-time systems having magnitude and rate-bounded actuators

Kucukdemiral, Ibrahim; Han, Xiaoran; Erden, Mustafa Suphi

Published in:
ISA Transactions

DOI:
10.1016/j.isatra.2022.02.025

Publication date:
2022

Document Version
Publisher's PDF, also known as Version of record

ISA Transactions 129 (2022) 73–87

Contents lists available at ScienceDirect

ISA Transactions

journal homepage: www.elsevier.com/locate/isatrans

Research article

Robust induced $\ell_2 - \ell_\infty$ optimal control of discrete-time systems having magnitude and rate-bounded actuators

Ibrahim Kucukdemiral [a,*], Xiaoran Han [b], Mustafa Suphi Erden [b]

[a] Glasgow Caledonian University, School of Computing, Engineering and Built Environment, Department of Applied Science, Glasgow, UK
[b] Heriot-Watt University, Institute of Sensors, Signals and Systems, Edinburgh, UK

ARTICLE INFO

Article history:
Received 30 June 2021
Received in revised form 13 February 2022
Accepted 13 February 2022
Available online 22 February 2022

Keywords:
Robust control
Magnitude and rate-bounded systems
Discrete-time systems
LMIs

ABSTRACT

The design of robust state- and output-feedback control for uncertain discrete-time systems with physical magnitude and rate constraints on their actuator dynamics was addressed. Unlike the traditional methods such as anti-windup (AW) methods, nested ellipsoids, model predictive controllers (MPCs) and integral quadratic constraints(IQCs) formulated by sector bounded inequalities, this paper uses a transformation of the system dynamics to a form which considers control signal and its rate as controlled outputs and using discrete-time ℓ_∞ induced (peak-to-peak) norm from disturbance inputs to these outputs. To cope with the magnitude and rate bound non-linearities together, the induced ℓ_∞ norm from disturbance input to the outputs involving control signal and its rate is utilised. On the other hand, discrete-time(DT) induced ℓ_2 norm from disturbance input to the main controlled output is used to mitigate the effects of disturbances. We can tackle this ambitious non-linear control problem in the domain of linear convex multi-objective optimal control problem, which can be solved by effective semi-definite optimisation methods by using the proposed transformation and handling the control constraints in terms of worst case peak-to-peak gain of the system. Extended Linear Matrix Inequalities (LMIs) and full block S-procedure based design conditions developed over Linear Fractional Representation(LFR) framework allow the user to obtain robust state- and output-feedback control solutions with reduced conservatism. For the first time, this paper introduces an extended LMI based robust output-feedback control design for magnitude and rate bounded (MRB) systems, using full block S-procedure. We demonstrate the performance of the proposed controller through several simulations over benchmark examples covering systems having multi-variable structures and uncertainties. Our study also involves comparison results with a recently introduced technique based on multi-stage AW technique. The simulation results show that the proposed method of this paper is much effective and less conservative compared to the recent AW method provided in the literature.

1. Introduction

The industry is dominated by systems having actuators having physical limits, and those subjected to uncertainties and prejudicial disturbances. However, during control design, physical constraints on actuator dynamics are often ignored. However, magnitude, and particularly the rate-bounded actuators are prominent, perhaps inevitable in almost every control system. The problem is quite important, as complications might arise when the rate limits dominates the physics of the actuator [1]. These limitations might cause performance degradation or instability in transportation, sub-sea and aerospace processes, particularly those having mechanically restricted actuators. These disregarded limits might lead to serious consequences in several situations if they are ignored during the control design. For instance, the crash of YF-22 in 1992 was occurred as a result of control signal oscillations generated due to the slew-rate bounds on the aircraft manoeuvring actuators [2–7]. Other examples in MRB actuators act as a source of loss of performance or even stability include the control of jet engine compressors [8], active fins in vessel stabilisation [9], vibration control for aerial refuelling hoses [10], and general reaction processes with sluggish actuators [11].

Hence, developing high performance robust controllers for processes having actuators with limited capacity has been a fundamental challenge for control theorists and practitioners for a long-time [12]. The literature is rich for processes having only magnitude bounded actuators [13–16], and the problem is widely addressed by using AW controllers [14,17–19]. However, the research on rate-limited actuators is restricted in comparison to the extensive literature on the control issue of systems with

* Corresponding author.
E-mail addresses: ibrahim.kucukdemiral@gcu.ac.uk (I. Kucukdemiral), hxr807@hotmail.com (X. Han), m.s.erden@hw.ac.uk (M.S. Erden).

https://doi.org/10.1016/j.isatra.2022.02.025

just magnitude limited control inputs. Different solutions to the problem exists depending on the nature of the process controlled. For systems with non-linear dynamics, for instance, a continuous-time (CT) model predictive control(MPC) approach is proposed in [20], to obtain a non-linear constrained control law that ensured a strict satisfaction of input rate and magnitude constraints. Non-linear control schemes based on Linear Parameter Varying (LPV) modelling are also proposed by [21,22]. Tohidi et al. [23] developed a new projection based adaptive control strategy for uncertain over actuated systems with MRB actuators. Attractive ellipsoidal method (AEM) has also been widely studied in robust control design for uncertain non-linear systems [24–28] including those with bounded actuators. However, AEM is generally used in the control of a class of stationary systems and this leads to a hard restriction on the design method. Moreover, the generic approach of the technique is essentially restricted to a subclass of system models characterised by ordinary differential equations (ODEs) in quasi-Lipschitz form [29]. A non-linear sliding mode controller is developed for single-input, single-output linear systems subject to bounded disturbances [30]. Their approach solves the problem using state-dependent parameters and involves an implementation in DT domain. Later, their proposed control methodology is extended and implemented on the pitch control problem of wind turbines, [31]. A new sliding-mode state feedback control method is also considered for linear systems subject to norm-bounded disturbances [32]. However, the proposed method is not applicable to systems having uncertainties.

In the linear control setting, the problem is generally addressed by using MPC which is a well-established technique for dealing with cross-correlated MIMO systems having stringent input/output constraints. However, increased real-time computational complexity, the requirement for an accurate system model, associated stability challenges, robustness of the closed-loop system under model mismatch, infeasibility that may arise during the real-time solution of the optimisation problem, and the requirement for large storage space and fast processors make them unsuitable for use in cheap and fast applications; especially those with uncertain parameters and subject to fast disturbance effects [9,33].

Another group utilises modified versions of AW techniques. An extensive overview of the modern approaches of this category are summarised in the literature [1]. In this approach, constraints on manipulated variables are not considered in the initial design, but later used as an add-on system to mitigate the unfavourable effects of constraints by introducing correction blocks into the feedback loop. First, a linear controller is developed without taking into account the saturation non-linearities throughout the design. Then, a so-called AW controller is introduced to the feedback interconnection to tackle with the input saturation constraints. Therefore, the technique requires huge effort and practically difficult to implement, especially when the controlled system is uncertain and has both MRB constraints. For example, [34], presents an innovative technique for overcoming the difficulty that employs integrating blocks with saturation non-linearity and various AW interconnection. The proposed approach considers the $\mathcal{L}_2$ gain objective between the plant output and the disturbance. However, this work does not consider uncertainties in the system model and the proposed controller is only applicable to CT processes. [35] introduces a new controller that uses the rate-of-change of the system outputs along with the AW structure. Their method is based on the LMI tools and generalised sector conditions. This approach also does not consider the robust control problem and it is limited to CT processes. For MRB systems affected by norm-bounded external disturbances, a novel AW based control technique is suggested [36]. To suppress the conservatism arising from the LMI relaxations employed, and to achieve a better control execution, a group of multi-staged AW architectures has been proposed in the paper. However, they do not consider the analysis of robustness of their approach.

A different group addresses the problem by representing the saturation non-linearity by convex hulls. The slew-rate and magnitude limits are represented with nested blocks [37–40]. Among them, [38,40] consider the problem in DT domain. Nevertheless, they do not consider disturbance attenuation problem. Recently, the problem is also considered in the domain of attractive and nested ellipsoids by [6]. However, the method is only applicable to state-feedback control. The last group approaches the problem by using a fixed low-order model to depict physical bounds on the dynamics.and then design controllers by minimising some induced gains related with the performance of the closed-loop system [41–43]. Again, these papers do not consider the robustness and these techniques are only applicable to CT processes.

In accordance with our discussion above, within the limited number of research papers that consider MRB simultaneously, most of the results in the literature are based on MPCs, non-linear control methods, attractive ellipsoids and AW based techniques and their derivatives. MPCs and non-linear control methods are generally difficult to implement, whereas the attractive ellipsoid methods are not very suitable for output-feedback. On the other hand, AW based methods rarely consider the robustness of the control scheme. They are mostly obtained in CT setting and might excite high frequency vibrations on the actuator mechanism due to ringing problem. These harmonics might generate devastating effects in long run and may lead to wearing and tearing, component failures, and therefore abnormalities during prolonged use. Finally, as also stressed by [1], the AW techniques which can be found in the literature today have evolved from many sources and, even now, there is no unified approach; they are very diverse and somewhat disconnected from each other.

Because the reasons mentioned above, the goal of this research is to develop a reliable DT output-feedback controller for systems with MRB actuators that are subjected to norm-bounded disturbances. This study contributes to the current literature in a variety of ways. To begin, the approach suggested in this note is based on multi-parameter optimisation and augmented form representation of the process. Three separate controllable outputs are present in the enhanced plant representation. The peak-to-peak (induced ℓ_∞) gain from the disturbance inputs to the outputs created by the control signal and its rate is used to handle actuator saturation. The induced ℓ_2 norm of the closed-loop system is employed to attenuate disturbances via a third regulated output. A similar approach is employed in CT domain in [7]. The use of the proposed transformation and multi-objective norm considerations, help us deal with this challenging non-linear control problem in the context of linear convex multi-objective optimisation. The solution proposed in this paper can be considered as a major extension of the continuous-time state-feedback control method introduced in the author's recent paper [7] to the robust dynamic output-feedback control in discrete-time domain. To achieve this goal, we have exploited from the matrix transformations used in [44] which have been proven to be minimally conservative.

Since the proposed method provides a control signal that never saturates by keeping the operation in linear region, a mild activity is always guaranteed. Unlike its AW counterpart, the proposed approach in this article is highly convenient to utilise in mechanically actuated systems that may fail due to demanding working conditions and heavy usage. In contrast to the AW mechanism, the suggested controller is designed in a single try.

It is well known that the solutions to multi-objective optimal control problems are generally conservative due to the

restrictions on the usage of common Lyapunov matrices during the design. All design methods introduced in this paper are based on extended LMIs and therefore, the control solutions are independent of the Lyapunov matrices which helps user to introduce independent Lyapunov matrices for separate LMI conditions leading to less conservative results.

Finally, we extend the proposed nominal state- and output-feedback design techniques to the control of processes having uncertainties. In order to generate controllers with decreased conservatism, the robust controller synthesis techniques presented in this note are based on the full block S-procedure and dilated LMIs [45]. LFR of the system dynamics and P'olya relaxation are used to deal with its uncertainties. Therefore, the proposed robust control method is applicable to any system with uncertainties in the form of rational parameter dependence. Existing techniques cannot cope with the problem without introducing additional conservatism to the solution. To the best of authors knowledge, for the first time, this paper introduces an extended LMI based robust output-feedback control design using full block S-procedure.

This paper is structured as follows: Next section provides the statement of the control problem considered in this paper. Then, in Section 3, design methods are presented for full state- and output-feedback control problems considering the nominal and uncertain cases respectively. The effectiveness of the proposed controllers are demonstrated by simulation of different examples in Section 4. During the simulation studies, 2 different systems having hard input constraints and uncertainties are considered. One of the provided examples demonstrates the effectiveness of our approach by providing comparison results with multi-stage AW controller proposed in [36] and $\mathcal{H}_\infty$ controller from the literature. Finally, Section 5 concludes this paper.

Notation:. Respectively, $\mathbb{N}$, $\mathbb{R}$ and $\mathbb{Z}$ show the sets of natural, real and integer numbers. The notation $\mathbb{R}^+$ is reserved for the set of positive real scalars. $\mathbb{R}^n$ shows real vectors with dimension n, and $\mathbb{R}^{x\times y}$ denotes $x \times y$ sized real matrices. I is the representation of identity matrices and $\mathbf{0}$ is used for null matrices. G^T symbolises the transpose of the matrix G. $\mathrm{He}\{M\} = M + M^T$. $\star$ is used in symmetric matrices to represent off-diagonal symmetric blocks. For a vector of vectors z, $z_j^i(k) \in \mathbb{R}$ shows the ith term of the jth vector component of the vector z. $\bar{u}_i$ is a known scalar that stands for the magnitude limit of the ith control port of the signal u, and $\bar{v}_i$ shows the corresponding rate limit. For a vector signal w, $\|w\|_2$ is its 2-norm and $\|w\|_\infty$ represents its infinity norm. In this paper, we define $\|w\|_\infty \triangleq \max_{1\le j\le n_w} \sup_{k\ge 0} |w_j(k)|$. $\mathrm{diag}\{\cdot\}$ is used to represent diagonal matrices with matrix entries on its diagonal. $\mathrm{conv}\{\mathcal{S}\}$ symbolises the convex hull of the set $\mathcal{S}$. $A \succ (\prec) \mathbf{0}$ means all eigenvalues of A are real and positive (negative). $\mathbf{1}_{x,y}$ is a row vector whose xth and yth entries are 1 and all other entries are null. Similarly, $\mathbf{1}_x$ is a row vector whose xth entry is 1 and all other entries are 0. $\mathbf{H}_{y,r}$ is the transfer function from input r to output y and $\|\mathbf{H}\|_x$ is its induced $x-$ norm.

2. Problem formulation

Consider the stabilisable and detectable DT uncertain system represented by

$$\begin{aligned} x(k+1) &= A(\Delta(k))x(k) + B(\Delta(k))u(k) + H(\Delta(k))w(k),\\ z_1(k) &= C_{z1}x(k) + D_{z1}u(k) + D_{z2}w(k)\\ y(k) &= C_y x(k) + D_{y2}w(k) \end{aligned} \tag{1}$$

where $z_1(k) \in \mathbb{R}^{p_{z1}}$ is the exogenous(performance) output that is controlled. $y(k) \in \mathbb{R}^{p_y}$ is the measurement, and $x(k) \in \mathbb{R}^n$ is the state vector of the plant which satisfies $x(0) = \mathbf{0}$ and $w_k \in \mathbb{R}^{n_w}$ is an energy- and peak-bounded unknown disturbance signal that meets the condition $w^T(k)w(k) \le \|w\|_\infty^2$ for every $k \ge 0$. The standing assumption is that the peak value $\|w\|_\infty \in \mathbb{R}^+$ is available. $A(\Delta(k))$, $B(\Delta(k))$ and $H(\Delta(k))$ are time-varying, uncertain system matrices. $\Delta(k) \in \mathbf{\Delta}$ shows the time-varying unknown parameter matrix at the time instant $k \ge 0$ with $\mathbf{\Delta}$ being a known bounding set. $\forall k \ge 0$, and considering $\bar{u}_i$ and $\bar{v}_i$ are symmetric and known limits for the ith channel of the control, the manipulating signal $u(k) \in \mathbb{R}^m$ has the following physical limits for its channels $i = 1, \ldots, m$:

$$|u_i(k)| \le \bar{u}_i, \qquad |v_i(k)| \triangleq |u_i(k) - u_i(k-1)| \le \bar{v}_i,\ u_i(-1) = 0. \tag{2}$$

We aim to find robust full state- and dynamic output-feedback controllers for (1) that satisfy the magnitude and rate bounds given in (2) for any time instant k, while attenuating the disturbance $w(k)$ on the controlled output vector $z_1(k)$ in terms of minimum achievable induced ℓ_2 gain, γ_∞.

3. Main results

3.1. Nominal induced ℓ_2/ℓ_∞ control

We will start with the nominal control problem where all of the system matrices in (1) are assumed to be known and constant at their nominal values. The system is subject to peak- and energy-bounded disturbances and its control input suffers from hard magnitude and rate constraints as described in (2). The proposed method of this paper ensures full conformity to these bounds using peak-to-peak gain of the closed-loop system. Therefore, in an effort to derive a multi-objective optimisation based solution that relies on the peak-to-peak and energy-to-energy gain of the closed-loop system, the control signal itself and its rate will be considered as augmented state vector components. Then, the manipulating variable of the augmented system will be taken as the change in the rate of the control signal. This augmentation can be considered as an extension of the well-known velocity form representation of linear time-invariant systems [46] to acceleration form.

Now consider the DT system (1), with control signal constraints (2). Note that using accumulation chains, one can always write $u(k)$ as $u(k) = u(k-1) + v(k)$ where $v(k) = v(k-1) + \mu(k)$. Here, the initial values of control-related signals are taken as zero, i.e. $u(-1) = v(-1) = 0$. Then, according to system representation (1), one can write

$$\begin{bmatrix} x(k+1)\\ u(k)\\ v(k) \end{bmatrix} = \underbrace{\begin{bmatrix} A & B & B\\ \mathbf{0} & I & I\\ \mathbf{0} & \mathbf{0} & I \end{bmatrix}}_{\mathcal{A}} \underbrace{\begin{bmatrix} x(k)\\ u(k-1)\\ v(k-1) \end{bmatrix}}_{\bar{x}(k)} + \underbrace{\begin{bmatrix} B\\ I\\ I \end{bmatrix}}_{\mathcal{B}} \mu(k) + \underbrace{\begin{bmatrix} H\\ \mathbf{0}\\ \mathbf{0} \end{bmatrix}}_{\mathcal{H}} w(k), \tag{3}$$

where, $\mu(k)$ can be considered as the new artificial control signal for the augmented system (3), or an auxiliary control signal of (1). As a result of this modification, we may now define u and v as new extended states. Together with the initial controlled output z_1, we can incorporate additional controlled outputs $z_2 \triangleq u(k)$ and $z_3 \triangleq v(k)$. Then, whenever $\bar{u}_i$ and $\bar{v}_i$ of the ith channel of the control vector are given, and $\|w\|_\infty$ is known, one can impose the following conditions

$$\frac{\|z_2^i\|_\infty}{\|w\|_\infty} = \frac{\bar{u}_i}{\|w\|_\infty}, \quad i = 1, \ldots, m, \tag{4}$$

and

$$\frac{\|z_3^i\|_\infty}{\|w\|_\infty} = \frac{\bar{v}_i}{\|w\|_\infty}, \quad i = 1, \ldots, m. \tag{5}$$

Hence, $\mu(k)$, and thus the control signal $u(k)$, are determined to suppress the disturbing signal w on the controlled output z_1 and satisfaction of the restrictions (4) and (5) make the control signal and its derivate never exceed the magnitude and rate bounds (2). Once the auxiliary control signal $\mu(k)$ is obtained, then one can retrieve $u(k)$ readily by using the last two rows of the equality (3) as follows:

$$\begin{aligned} u(k) &= u(k-1) + v(k), \\ v(k) &= v(k-1) + \mu(k), \quad u(-1) = v(-1) = 0. \end{aligned} \tag{6}$$

Now, following the augmentation (3), as an ingredient to the solution of the afore-mentioned control problem described in Section 2, we define the following performance outputs:

$$\begin{bmatrix} z_1(k) \\ z_2^i(k) \\ z_3^i(k) \end{bmatrix} = \begin{bmatrix} \mathcal{C}_{z1} \\ \mathcal{C}_{z2}^i \\ \mathcal{C}_{z3}^i \end{bmatrix} \bar{x}(k) + \begin{bmatrix} \mathcal{D}_{z11} \\ \mathcal{D}_{z21}^i \\ \mathcal{D}_{z31}^i \end{bmatrix} \mu(k) + \begin{bmatrix} \mathcal{D}_{z12} \\ \mathcal{D}_{z22}^i \\ \mathcal{D}_{z32}^i \end{bmatrix} w(k), \tag{7}$$

where $i = 1, \ldots, m$. Considering the ith control channel of the system dynamics (1), the matrices of the performance outputs can be represented compactly as $\mathcal{C}_{z1} = \begin{bmatrix} C_{z1} & D_{z1} & D_{z1} \end{bmatrix}$, $\mathcal{D}_{z11} = D_{z1}$, $\mathcal{D}_{z12} = D_{z2}$, $\mathcal{C}_{z2}^i = \mathbf{1}_{n+i,n+m+i}$, $\mathcal{C}_{z3}^i = \mathbf{1}_{n+m+i}$, $\mathcal{D}_{z21}^i = \mathcal{D}_{z31}^i = \mathbf{1}_i$, $\mathcal{D}_{z22}^i = \mathbf{0}$ and $\mathcal{D}_{z32}^i = \mathbf{0}$ where, $i = 1, \ldots, m$. Finally, based on the augmentation (3), the measured outputs can be defined as

$$\underbrace{\begin{bmatrix} y(k) \\ u(k-1) \\ v(k-1) \end{bmatrix}}_{\bar{y}(k)} = \underbrace{\begin{bmatrix} C_y & \mathbf{0} & \mathbf{0} \\ \mathbf{0} & I & \mathbf{0} \\ \mathbf{0} & \mathbf{0} & I \end{bmatrix}}_{\mathcal{C}_y} \bar{x}(k) + \underbrace{\begin{bmatrix} D_{y2} \\ \mathbf{0} \\ \mathbf{0} \end{bmatrix}}_{\mathcal{D}_y} w(k). \tag{8}$$

Our aim is to find a control law either in the form of $u(k) = f(\bar{x}(k))$ for a full state-feedback controller, or $u(k) = f(\bar{y}(k))$ for a dynamic output-feedback controller that minimise the induced ℓ_2 gain, $\gamma_\infty \triangleq \|\mathbf{H}_{z_1,w}\|_{\ell_2 \leftarrow \ell_2}$ and satisfy the magnitude and rate constraints on the control signal defined in (2). As outlined above, one approach would be to seek for minimum gain γ_∞ and satisfy $\|\mathbf{H}_{z_2^i,w}\|_{\ell_\infty \leftarrow \ell_\infty} = \bar{u}_i/\|w\|_\infty$ and $\|\mathbf{H}_{z_3^i,w}\|_{\ell_\infty \leftarrow \ell_\infty} = \bar{v}_i/\|w\|_\infty$ for every $i = 1, \ldots, m$.

To this end, based on extended matrix inequalities, we propose Lemma 1 below, which provides a method for calculation of the worst case value of the peak-to-peak gain, $\|\mathbf{H}_{z,w}\|_{\ell_\infty \leftarrow \ell_\infty}$ for a linear time-invariant DT system defined by

$$\begin{aligned} \bar{x}(k+1) &= \mathcal{A}_{cl}\bar{x}(k) + \mathcal{B}_{cl}w(k) \\ z(k) &= \mathcal{C}_{cl}\bar{x}(k) + \mathcal{D}_{cl}w(k), \end{aligned} \tag{9}$$

where $w^T(k)w(k) \leq \|w\|_\infty^2$. Depending on the type of the control -full state-feedback/output-feedback-, the closed-loop matrices in (9) will take different forms as will be discussed in the subsequent sections. Lemma 1 can be considered as an extension of the results of [47] to the extended matrix inequalities as an attempt to find a less-conservative solution to the multi-objective optimisation problem outlined above. Expressing the peak-to-peak gain conditions in the form of extended LMIs help us utilise the condition efficiently in multi-objective control problems with marginal added conservatism.

Lemma 1. *If there exist a symmetric matrix $X \succ 0$, matrix G and positive constants ρ and $\lambda \in (0, 1)$ such that:*

$$\begin{bmatrix} G + G^T - X & \mathcal{A}_{cl}G & \mathcal{B}_{cl} \\ G^T\mathcal{A}_{cl}^T & (1-\lambda)X & \mathbf{0} \\ \mathcal{B}_{cl}^T & \mathbf{0} & \rho I \end{bmatrix} \succ \mathbf{0}, \tag{10}$$

and

$$\begin{bmatrix} \lambda X & \mathbf{0} & \star \\ \mathbf{0} & (\alpha-\rho)I & \star \\ \mathcal{C}_{cl}G & \mathcal{D}_{cl} & \alpha I \end{bmatrix} \succ \mathbf{0}, \tag{11}$$

then, system (9) is asymptotically stable and $\|\mathbf{H}_{z,w}\|_{\ell_\infty \leftarrow \ell_\infty} < \alpha$.

Proof. Let us consider a Lyapunov function $V(\bar{x}(k)) = \bar{x}^T(k)P^{-1}\bar{x}(k)$ along the trajectory (9) where $P = P^T \succ 0$. Assume that $V(\bar{x}(k))$ satisfies

$$V(\bar{x}(k+1)) - V(\bar{x}(k)) + \lambda V(\bar{x}(k)) - \rho w(k)^T w(k) < 0, \tag{12}$$

for all $k \geq 0$ and some positive numbers $\lambda \in (0, 1)$ and ρ. Hence, based on the selection of the Lyapunov function, the inequality (12) can be rewritten as

$$\bar{x}^T(k+1)P^{-1}\bar{x}(k+1) + (\lambda-1)\bar{x}^T(k)P^{-1}\bar{x}(k) - \rho w^T(k)w(k) < 0. \tag{13}$$

On the other hand, based on the closed-loop system trajectory (9), for every invertible matrix G and $\forall k \geq 0$, one can write a null equation

$$2\bar{x}^T(k+1)G^{-T}\left(\bar{x}(k+1) - \mathcal{A}_{cl}\bar{x}(k) - \mathcal{B}_{cl}w(k)\right) = 0. \tag{14}$$

Therefore, (13) can be rewritten as

$$\begin{aligned} &\bar{x}^T(k+1)P^{-1}\bar{x}(k+1) + (\lambda-1)\bar{x}^T(k)P^{-1}\bar{x}(k) \\ &-\rho w^T(k)w(k) - 2\bar{x}^T(k+1)G^{-T}\left(\bar{x}(k+1)\right. \\ &\left. - \mathcal{A}_{cl}\bar{x}(k) - \mathcal{B}_{cl}w(k)\right) < 0, \end{aligned} \tag{15}$$

which can be further written in compact form as follows:

$$\begin{bmatrix} \bar{x}(k+1) \\ \bar{x}(k) \\ w(k) \end{bmatrix}^T \begin{bmatrix} P^{-1} - G^{-1} - G^{-T} & G^{-T}\mathcal{A}_{cl} & G^{-T}\mathcal{B}_{cl} \\ \mathcal{A}_{cl}^T G^{-1} & (\lambda-1)P^{-1} & \mathbf{0} \\ \mathcal{B}_{cl}^T G^{-1} & \mathbf{0} & -\rho I \end{bmatrix} \times \begin{bmatrix} \bar{x}(k+1) \\ \bar{x}(k) \\ w(k) \end{bmatrix} < 0. \tag{16}$$

Therefore, pre- and post-multiplying the middle multiplier matrix in (16) by $\mathrm{diag}\{G^T, G^T, I\}$ and its transpose, respectively, yield

$$\begin{bmatrix} G^TP^{-1}G - G - G^T & \mathcal{A}_{cl}G & \mathcal{B}_{cl} \\ G^T\mathcal{A}_{cl}^T & (\lambda-1)G^TP^{-1}G & \mathbf{0} \\ \mathcal{B}_{cl}^T & \mathbf{0} & -\rho I \end{bmatrix} \prec \mathbf{0}. \tag{17}$$

Then, defining $X \triangleq G^TP^{-1}G$, condition (17) is equivalent to (10), which also guarantees asymptotic stability.

Let us recall (12) and define an extreme Lyapunov function $\bar{V}(\bar{x}(k)) \triangleq V(\bar{x}(k))$ which satisfies

$$\bar{V}(k+1) = (1-\lambda)\bar{V}(k) + \rho w(k)^T w(k). \tag{18}$$

Note that the solution to this first order difference equation can be written as

$$\bar{V}(k) = \sum_{j=0}^{k-1} \underbrace{(1-\lambda)^j}_{s^j} \rho w(k-1-j)^T w(k-1-j). \tag{19}$$

However, since $w^T(k)w(k) \leq \|w\|_\infty^2$ for all $k \geq 0$, $\bar{V}(k) \leq \sum_{j=0}^{k-1} s^j \rho \|w\|_\infty^2$. On the other hand, since $0 < \lambda < 1$ and $\sum_{j=0}^{k-1} s^j = \frac{1-s^k}{1-s}$, this further implies

$$\begin{aligned} V(\bar{x}(k)) &= \bar{x}^T(k)P^{-1}\bar{x}(k) \\ &\leq \rho \frac{1-s^k}{1-s}\|w\|_\infty^2 \\ &= \rho \frac{1-(1-\lambda)^k}{\lambda}\|w\|_\infty^2. \end{aligned} \tag{20}$$

Besides, let

$$\begin{bmatrix} \mathcal{C}_{cl} & \mathcal{D}_{cl} \end{bmatrix}^T \frac{1}{\alpha} \begin{bmatrix} \mathcal{C}_{cl} & \mathcal{D}_{cl} \end{bmatrix} \prec \begin{bmatrix} \lambda P^{-1} & \mathbf{0} \\ \mathbf{0} & (\alpha-\rho)I \end{bmatrix}. \tag{21}$$

According to (20), one can conclude that

$$z^T(k)z(k) = (\mathcal{C}_{cl}\bar{x}(k) + \mathcal{D}_{cl}w(k))^T(\mathcal{C}_{cl}\bar{x}(k) + \mathcal{D}_{cl}w(k))$$

$$
\begin{aligned}
&= \begin{bmatrix} \bar{x}(k) \\ w(k) \end{bmatrix}^T \begin{bmatrix} \mathcal{C}_{cl}^T \mathcal{C}_{cl} & \mathcal{C}_{cl}^T \mathcal{D}_{cl} \\ \mathcal{D}_{cl}^T \mathcal{C}_{cl} & \mathcal{D}_{cl}^T \mathcal{D}_{cl} \end{bmatrix} \begin{bmatrix} \bar{x}(k) \\ w(k) \end{bmatrix} \\
&\leq \alpha(\lambda \bar{x}^T(k) P^{-1} \bar{x}(k) + (\alpha - \rho) w^T(k) w(k)) \\
&\leq \alpha \left((1 - (1-\lambda)^k) \rho \|w\|_\infty^2 + (\alpha - \rho) \|w\|_\infty^2 \right) \\
&\leq \alpha \left(\rho \|w\|_\infty^2 + (\alpha - \rho) \|w\|_\infty^2 \right) \\
&= \alpha^2 \|w\|_\infty^2, \qquad (22)
\end{aligned}
$$

which further implies $\|z\|_\infty^2 / \|w\|_\infty^2 < \alpha^2$. Note that, based on the Schur complement formula [48], matrix inequality (21) is equivalent to

$$
\begin{bmatrix} \lambda P^{-1} & \mathbf{0} & \mathcal{C}_{cl}^T \\ \star & (\alpha - \rho) I & \mathcal{D}_{cl}^T \\ \star & \star & \alpha I \end{bmatrix} \succ \mathbf{0}. \qquad (23)
$$

Then, pre- and post-multiplying (23) by $\mathrm{diag}\{G^T, I, I\}$ and its transpose, respectively and using the definition $X \triangleq G^T P^{-1} G$ whenever it is applicable, gives (11). Finally, the positive definiteness of the upper left 2 by 2 block of the inequality (10) guarantees the asymptotic stability of the generic system (9). This concludes the proof.

Remark 1. In order to find a solution to (10) and (11), a line search over $\lambda \in (0, 1)$ is needed. This is also needed to reduce conservatism and increase the dimension of the solution space.

Theorem 1 (*[44]*). *The inequality $\|\mathbf{H}_{z,w}\|_{\ell_2 \leftarrow \ell_2} < \gamma_\infty$ holds for (9) if, and only if, there exist a matrix G, a symmetric matrix $W \succ 0$ in appropriate dimensions and a positive real number γ_∞ which satisfy*

$$
\begin{bmatrix} W & \mathcal{A}_{cl} G & \mathcal{B}_{cl} & \mathbf{0} \\ G^T \mathcal{A}_{cl}^T & G + G^T - W & \mathbf{0} & G^T \mathcal{C}_{cl}^T \\ \mathcal{B}_{cl}^T & \mathbf{0} & I & \mathcal{D}_{cl}^T \\ \mathbf{0} & \mathcal{C}_{cl} G & \mathcal{D}_{cl} & \gamma_\infty^2 I \end{bmatrix} \succ 0. \qquad (24)
$$

3.1.1. Full state-feedback control

The following theorem provides a nominal full state-feedback control solution to the problem mentioned in Section 2. The solution requires the full-state measurement.

Theorem 2. *Consider system (1) with controlled outputs (7). The system is subjected to magnitude and rate constraints as given in (2). Given the positive real numbers γ_∞ and $\lambda \in (0, 1)$, and based on the definition of augmented system matrices in (3), there exists a full state-feedback controller of the form (6) where $\mu(k) = K \underbrace{\begin{bmatrix} x^T(k) & u^T(k-1) & v^T(k-1) \end{bmatrix}^T}_{\bar{x}^T(k)}$, satisfying $\|\mathbf{H}_{z_1,w}\|_{\ell_2 \leftarrow \ell_2} < \gamma_\infty$ and the magnitude and rate constraints given in (2), if there exist $\rho > 0$ and matrices $X = X^T \succ \mathbf{0}$, $W = W^T \succ \mathbf{0}$, L and G which satisfy the following matrix inequalities for all $i = 1, \ldots, m$:*

$$
\begin{bmatrix} G + G^T - X & \star & \star \\ G^T \mathcal{A}^T + L^T \mathcal{B}^T & (1-\lambda) X & \star \\ \mathcal{H}^T & \mathbf{0} & \rho I \end{bmatrix} \succ \mathbf{0}, \qquad (25)
$$

$$
\begin{bmatrix} \lambda X & \star & \star \\ \mathbf{0} & \left(\frac{\bar{u}_i}{\|w\|_\infty} - \rho \right) I & \star \\ \mathcal{C}_{z2}^i G + \mathcal{D}_{z21}^i L & \mathbf{0} & \frac{\bar{u}_i}{\|w\|_\infty} I \end{bmatrix} \succ \mathbf{0}, \qquad (26)
$$

$$
\begin{bmatrix} \lambda X & \star & \star \\ \mathbf{0} & \left(\frac{\bar{v}_i}{\|w\|_\infty} - \rho \right) I & \star \\ \mathcal{C}_{z3}^i G + \mathcal{D}_{z31}^i L & \mathbf{0} & \frac{\bar{v}_i}{\|w\|_\infty} I \end{bmatrix} \succ \mathbf{0}, \qquad (27)
$$

and

$$
\begin{bmatrix} W & \mathcal{A}G + \mathcal{B}L & \mathcal{H} & \mathbf{0} \\ \star & G + G^T - W & \mathbf{0} & G^T \mathcal{C}_{z1}^T + L^T \mathcal{D}_{z11}^T \\ \star & \star & I & \mathcal{D}_{z12}^T \\ \star & \star & \star & \gamma_\infty^2 I \end{bmatrix} \succ \mathbf{0}. \qquad (28)
$$

Then, the feedback control gain can be recovered as $K = LG^{-1}$.

Proof. Consider the augmented system formulation (3). Since there are two constraints on the magnitude of u and v, we consider two independent peak-to-peak gains, $\bar{u}_i / \|w\|_\infty$ and $\bar{v}_i / \|w\|_\infty$ for the control channels $i = 1, \ldots, m$ with the common Lyapunov matrix $P \succ 0$. Therefore, based on the results of Lemma 1 and choosing $z_2(k) = u(k)$ and $z_3(k) = v(k)$ in (7), feasibility of the conditions (25), (26) and (27) guarantee that the control signals never saturate in terms of the magnitude and rate bounds stated in (2). In Lemma 1, using the matrix definitions $\mathcal{A}_{cl} = \mathcal{A} + \mathcal{B}K$, $\mathcal{B}_{cl} = \mathcal{H}$, $\mathcal{C}_{cl} = \mathcal{C}_{z2}^i + \mathcal{D}_{z21}^i K$ along with the definition $L \triangleq KG$ and choosing $\alpha = \bar{u}_i / \|w\|_\infty$ leads to (26). Similarly, using the matrix definition $\mathcal{C}_{cl} = \mathcal{C}_{z3}^i + \mathcal{D}_{z31}^i K$, choosing $\alpha = \bar{v}_i / \|w\|_\infty$ and using the definition of L in its place, gives (27). Finally, using the definition of $K = LG^{-1}$ and replacing $\mathcal{A}_{cl}$ with $\mathcal{A} + \mathcal{B}K$, $\mathcal{B}_{cl}$ with $\mathcal{H}$, $\mathcal{C}_{cl}$ with $\mathcal{C}_{z1} + \mathcal{D}_{z11} K$ and $\mathcal{D}_{cl}$ with $\mathcal{D}_{z12}$ in (24) lead to (28). Note that based on Theorem 1, a feasible solution to (28) guarantees that $\|\mathbf{H}_{z_1,w}\|_{\ell_2 \leftarrow \ell_2} < \gamma_\infty$.

3.1.2. Output-feedback control

We shall consider a dynamic output-feedback control solution to the problem that we mentioned in Section 2. Since the problem involves multiple objectives, in order to synthesise a controller with minimal conservatism, we will employ a dilated LMI based solution. This will enable us to use independent Lyapunov functions for independent control objectives. To this end, in consideration of the augmented system model (3), exogenous outputs (7) and the measurement vector (8), let us define a feedback controller of the form

$$
\begin{aligned}
x_c(k+1) &= \mathcal{A}_c x_c(k) + \mathcal{B}_c \bar{y}(k) \\
\mu(k) &= \mathcal{C}_c x_c(k) + \mathcal{D}_c \bar{y}(k) \qquad (29)
\end{aligned}
$$

where $x_c \in \mathbb{R}^{n+2m}$ is the controller's state vector; $\mathcal{A}_c$, $\mathcal{B}_c$, $\mathcal{C}_c$ and $\mathcal{D}_c$ are the controller matrices with appropriate dimensions. Then, according to (3), (7), (8) and (29), we can define the closed-loop system dynamics as follows:

$$
\begin{aligned}
x_{cl}(k+1) &= \mathcal{A}_{cl} x_{cl}(k) + \mathcal{B}_{cl} w(k) \\
z(k) &= \mathcal{C}_{cl} x_{cl}(k) + \mathcal{D}_{cl} w(k) \qquad (30)
\end{aligned}
$$

where $x_{cl}(k) = \begin{bmatrix} \bar{x}^T(k) & x_c^T(k) \end{bmatrix}^T$ is the closed-loop state vector and

$$
\left[\begin{array}{c|c} \mathcal{A}_{cl} & \mathcal{B}_{cl} \\ \hline \mathcal{C}_{cl} & \mathcal{D}_{cl} \end{array}\right] = \left[\begin{array}{cc|c} \mathcal{A} + \mathcal{B}\mathcal{D}_c\mathcal{C}_y & \mathcal{B}\mathcal{C}_c & \mathcal{H} + \mathcal{B}\mathcal{D}_c\mathcal{D}_y \\ \mathcal{B}_c\mathcal{C}_y & \mathcal{A}_c & \mathcal{B}_c\mathcal{D}_y \\ \hline \mathcal{C}_z + \mathcal{D}_{z1}\mathcal{D}_c\mathcal{C}_y & \mathcal{D}_{z1}\mathcal{C}_c & \mathcal{D}_{z2} + \mathcal{D}_{z1}\mathcal{D}_c\mathcal{D}_y \end{array}\right]. \qquad (31)
$$

Now, without loss of generality, let us consider nominal augmented system (3) along with a generic controlled output

$$
z(k) = \mathcal{C}_z \bar{x}(k) + \mathcal{D}_{z1} \mu(k) + \mathcal{D}_{z2} w(k). \qquad (32)
$$

Here, depending on the input–output pairings, the size of control inputs and the existence of the magnitude and rate constraints on the control signal, one can assume that the controlled output matrices can take values in the form of $z(k) \in \{z_1(k), z_2^i(k), z_3^i(k)\}$, $\mathcal{C}_z \in \{\mathcal{C}_{z1}, \mathcal{C}_{z2}^i, \mathcal{C}_{z3}^i\}$, $\mathcal{D}_{z1} \in \{\mathcal{D}_{z11}, \mathcal{D}_{z21}^i, \mathcal{D}_{z31}^i\}$, and $\mathcal{D}_{z2} \in \{\mathcal{D}_{z12}, \mathcal{D}_{z22}^i, \mathcal{D}_{z32}^i\}$ where $i = 1, \ldots, m$.

The following Theorem 3 provides an extended LMI based induced ℓ_2/ℓ_∞ multi-objective dynamic output-feedback controller in the form (29) for the nominal augmented system (3) having

generic controlled output (32) and the measurements (8), to satisfy $\|\mathbf{H}_{z,w}\|_{\ell_2\leftarrow\ell_2} < \gamma_\infty$, $\|\mathbf{H}_{z,w}\|_{\ell_\infty\leftarrow\ell_\infty} < \alpha$. Later on, this theorem will constitute a basis for the output-feedback control solution to the problem described in Section 2.

Theorem 3. *Consider the augmented system (3) with the generic controlled output (32) and the measurement vector (8). Given the constants $\gamma_\infty > 0$ and $\lambda \in (0,1)$, there exists a dynamic output-feedback controller of the form (29), which satisfy $\|\mathbf{H}_{z,w}\|_{\ell_2\leftarrow\ell_2} < \gamma_\infty$, $\|\mathbf{H}_{z,w}\|_{\ell_\infty\leftarrow\ell_\infty} < \alpha$, if there exist scalars $\rho > 0$ and $\alpha > 0$, matrices $\mathsf{X} = \mathsf{X}^T \succ \mathbf{0}$, $M = M^T \succ \mathbf{0}$, $\mathsf{W} = \mathsf{W}^T \succ \mathbf{0}$, $E = E^T \succ \mathbf{0}$, G_{11}, J, S, W, R, N, F, Y, Z and Q which satisfy the following LMIs:*

$$\begin{bmatrix} G_{11}+G_{11}^T-\mathsf{X} & I+S^T-J & \mathcal{A}G_{11}+\mathcal{B}N & \mathcal{A}+\mathcal{B}R\mathcal{C}_y & \mathcal{H}+\mathcal{B}R\mathcal{D}_y \\ \star & Y+Y^T-M & Q & Y\mathcal{A}+F\mathcal{C}_y & Y\mathcal{H}+F\mathcal{D}_y \\ \star & \star & (1-\lambda)\mathsf{X} & (1-\lambda)J & \mathbf{0} \\ \star & \star & \star & (1-\lambda)M & \mathbf{0} \\ \star & \star & \star & \star & \rho I \end{bmatrix} \succ \mathbf{0}, \tag{33}$$

$$\begin{bmatrix} \lambda\mathsf{X} & \star & \star & \star \\ \lambda J^T & \lambda M & \star & \star \\ \mathbf{0} & \mathbf{0} & (\alpha-\rho)I & \star \\ \mathcal{C}_zG_{11}+\mathcal{D}_{z1}N & \mathcal{C}_z+\mathcal{D}_{z1}R\mathcal{C}_y & \mathcal{D}_{z2}+\mathcal{D}_{z1}R\mathcal{D}_y & \alpha I \end{bmatrix} \succ \mathbf{0}, \tag{34}$$

and

$$\begin{bmatrix} \mathsf{W} & Z & \mathcal{A}G_{11}+\mathcal{B}N & \mathcal{A}+\mathcal{B}R\mathcal{C}_y & \mathcal{H}+\mathcal{B}R\mathcal{D}_y & \mathbf{0} \\ \star & E & Q & Y\mathcal{A}+F\mathcal{C}_y & Y\mathcal{H}+F\mathcal{D}_y & \mathbf{0} \\ \star & \star & G_{11}+G_{11}^T-\mathsf{W} & I+S^T-Z & \mathbf{0} & (\mathcal{C}_zG_{11}+\mathcal{D}_{z1}N)^T \\ \star & \star & \star & Y+Y^T-E & \mathbf{0} & (\mathcal{C}_z+\mathcal{D}_{z1}R\mathcal{C}_y)^T \\ \star & \star & \star & \star & I & (\mathcal{D}_{z2}+\mathcal{D}_{z1}R\mathcal{D}_y)^T \\ \star & \star & \star & \star & \star & \gamma_\infty^2 I \end{bmatrix} \succ \mathbf{0}. \tag{35}$$

If a feasible solution set to the above inequalities exists, the controller matrices can be recovered as

$$\begin{bmatrix} \mathcal{A}_c & \mathcal{B}_c \\ \mathcal{C}_c & \mathcal{D}_c \end{bmatrix} = \begin{bmatrix} V^{-1} & -V^{-1}Y\mathcal{B} \\ \mathbf{0} & I \end{bmatrix} \begin{bmatrix} Q-Y\mathcal{A}G_{11} & F \\ N & R \end{bmatrix} \times \begin{bmatrix} G_{21}^{-1} & \mathbf{0} \\ -\mathcal{C}_yG_{11}G_{21}^{-1} & I \end{bmatrix}, \tag{36}$$

where V and G_{21} are any nonsingular matrices which satisfy $VG_{21} = S - YG_{11}$.

Proof. Similar to the procedure described in [44], let us introduce the following matrices: $\mathcal{K} \triangleq \begin{bmatrix} \mathcal{A}_c & \mathcal{B}_c \\ \mathcal{C}_c & \mathcal{D}_c \end{bmatrix}$, $G \triangleq \begin{bmatrix} G_{11} & ? \\ G_{21} & ? \end{bmatrix}$, $G^{-1} = \begin{bmatrix} Y^T & ? \\ V^T & ? \end{bmatrix}$ and $\mathbf{T} \triangleq \begin{bmatrix} I & Y^T \\ \mathbf{0} & V^T \end{bmatrix}$. Note that the matrices having entries ? are not important in the calculations. Also, let us define the following linearising transformations:

$$\begin{bmatrix} Q & F \\ N & R \end{bmatrix} \triangleq \begin{bmatrix} V & Y\mathcal{B} \\ \mathbf{0} & I \end{bmatrix} \mathcal{K} \begin{bmatrix} G_{21} & \mathbf{0} \\ \mathcal{C}_yG_{11} & I \end{bmatrix} + \begin{bmatrix} Y \\ \mathbf{0} \end{bmatrix} \mathcal{A} \begin{bmatrix} G_{11} & \mathbf{0} \end{bmatrix}, \tag{37}$$

$$\begin{bmatrix} \mathsf{X} & J \\ J^T & M \end{bmatrix} \triangleq \mathbf{T}^T X \mathbf{T}, \ \begin{bmatrix} \mathsf{W} & Z \\ Z^T & E \end{bmatrix} \triangleq \mathbf{T}^T W \mathbf{T}, \text{ and } S \triangleq YG_{11} + VG_{21}. \tag{38}$$

Using the matrix definitions given above, and the closed-loop matrices (31), one can obtain the following entry-wise linearising transformations:

$$\mathbf{T}^T\mathcal{A}_{cl}G\mathbf{T} = \begin{bmatrix} \mathcal{A}G_{11}+\mathcal{B}N & \mathcal{A}+\mathcal{B}R\mathcal{C}_y \\ Q & Y\mathcal{A}+F\mathcal{C}_y \end{bmatrix}, \tag{39}$$

$$\mathbf{T}^T\mathcal{B}_{cl} = \begin{bmatrix} \mathcal{H}+\mathcal{B}R\mathcal{D}_y \\ Y\mathcal{H}+F\mathcal{D}_y \end{bmatrix}, \tag{40}$$

$$\mathcal{C}_{cl}G\mathbf{T} = \begin{bmatrix} \mathcal{C}_zG_{11}+\mathcal{D}_{z1}N & \mathcal{C}_z+\mathcal{D}_{z1}R\mathcal{C}_y \end{bmatrix}, \tag{41}$$

$$D_{cl} = \begin{bmatrix} \mathcal{D}_{z2}+\mathcal{D}_{z1}\mathcal{R}\mathcal{D}_y \end{bmatrix}, \tag{42}$$

$$\mathbf{T}^T(G+G^T-X)\mathbf{T} = \begin{bmatrix} G_{11}+G_{11}^T & I+S^T \\ I+S & Y+Y^T \end{bmatrix} - \begin{bmatrix} \mathsf{X} & J \\ J^T & M \end{bmatrix}, \tag{43}$$

and

$$\mathbf{T}^T(G+G^T-W)\mathbf{T} = \begin{bmatrix} G_{11}+G_{11}^T & I+S^T \\ I+S & Y+Y^T \end{bmatrix} - \begin{bmatrix} \mathsf{W} & Z \\ Z^T & E \end{bmatrix}. \tag{44}$$

The linearisation transformation above requires the non-singularity of V and G_{21}. However, any feasible solution to (35) guarantees that

$$\begin{bmatrix} G_{11}+G_{11}^T & I+S^T \\ \star & Y+Y^T \end{bmatrix} \succ \begin{bmatrix} \mathsf{W} & Z \\ Z & E \end{bmatrix} \succ 0 \tag{45}$$

which implies that G_{11} and Y are nonsingular. Applying a congruence transformation on the left hand side of (45) by using a matrix $\begin{bmatrix} G_{11}^{-T} & -I \end{bmatrix}$ implies $\mathsf{He}\{(S-YG_{11})G_{11}^{-1}\} \prec 0$. Hence, $S-YG_{11}$ is non-singular. This proves that there exist nonsingular matrices V and G_{21} which satisfy $VG_{21} = S - YG_{11}$.

Then, in line with the closed-loop system matrix definitions given in (31) and the transformation matrices shown above, applying a congruence transformation on (10) using $\mathsf{diag}(\mathbf{T}, \mathbf{T}, I)$ yields (33). Similarly, applying a congruence transformation on (11) using $\mathsf{diag}(\mathbf{T}, I, I)$ gives (34). On the other hand, if we apply a congruence transformation on (24) with $\mathsf{diag}(\mathbf{T}, \mathbf{T}, I, I)$ leads to (35). Finally, we stress that V and G_{21} can simply be obtained by taking LU or QR factorisation of the matrix $(S - YG_{11})$. This is always possible since $(S - YG_{11})$ is nonsingular as explained above. Thus concludes our proof.

Following a similar procedure that we followed during the design of full-state feedback controller, we are in a position to propose the following result for a dynamic output-feedback solution to the constraint control problem presented in Section 2.

Corollary 4. *Consider nominal version of system (1) with controlled outputs (7), and the measurement vector (8). The system is subject to magnitude and rate constraints as shown in (2). Given the constants $\gamma_\infty > 0$ and $\lambda \in (0,1)$, and based on the definition of augmented system matrices in (3), there exists an output-feedback controller of the form (6) and*

$$\begin{aligned} x_c(k+1) &= \mathcal{A}_cx_c(k) + \mathcal{B}_c\bar{y}(k) \\ \mu(k) &= \mathcal{C}_cx_c(k) + \mathcal{D}_c\bar{y}(k) \end{aligned} \tag{46}$$

which satisfies the magnitude and rate constraints given in (2) and $\|\mathbf{H}_{z_1,w}\|_{\ell_2\leftarrow\ell_2} < \gamma_\infty$, if there exist a scalar $\rho > 0$ and matrices $\mathsf{X} = \mathsf{X}^T \succ \mathbf{0}$, $E = E^T \succ \mathbf{0}$, $M = M^T \succ \mathbf{0}$, $\mathsf{W} = \mathsf{W}^T \succ \mathbf{0}$, G_{11}, J, S, R, N, F, Y, Z and Q which satisfy (33) and the following matrix inequalities for each $i = 1, \ldots, m$:

$$\begin{bmatrix} \lambda\mathsf{X} & \star & \star & \star \\ \lambda J^T & \lambda M & \star & \star \\ \mathbf{0} & \mathbf{0} & (\bar{u}_i/\|w\|_\infty-\rho)I & \star \\ \mathcal{C}_{z2}^iG_{11}+\mathcal{D}_{z21}^iN & \mathcal{C}_{z2}^i+\mathcal{D}_{z21}^iR\mathcal{C}_y & \mathcal{D}_{z22}^i+\mathcal{D}_{z21}^iR\mathcal{D}_y & (\bar{u}_i/\|w\|_\infty)I \end{bmatrix} \succ \mathbf{0}, \tag{47}$$

$$\begin{bmatrix} \lambda\mathsf{X} & \star & \star & \star \\ \lambda J^T & \lambda M & \star & \star \\ \mathbf{0} & \mathbf{0} & (\bar{v}_i/\|w\|_\infty-\rho)I & \star \\ \mathcal{C}_{z3}^iG_{11}+\mathcal{D}_{z31}^iN & \mathcal{C}_{z3}^i+\mathcal{D}_{z31}^iR\mathcal{C}_y & \mathcal{D}_{z32}^i+\mathcal{D}_{z31}^iR\mathcal{D}_y & (\bar{v}_i/\|w\|_\infty)I \end{bmatrix} \succ \mathbf{0}, \tag{48}$$

$$\begin{bmatrix} W & Z & \mathcal{A}G_{11}+\mathcal{B}N & \mathcal{A}+\mathcal{B}R\mathcal{C}_y & \mathcal{H}+\mathcal{B}R\mathcal{D}_y & \mathbf{0} \\ \star & E & Q & Y\mathcal{A}+F\mathcal{C}_y & Y\mathcal{H}+F\mathcal{D}_y & \mathbf{0} \\ \star & \star & G_{11}+G_{11}^T-W & I+S^T-Z & \mathbf{0} & (\mathcal{C}_{z1}G_{11}+\mathcal{D}_{z11}N)^T \\ \star & \star & \star & Y+Y^T-E & \mathbf{0} & (\mathcal{C}_{z1}+\mathcal{D}_{z11}R\mathcal{C}_y)^T \\ \star & \star & \star & \star & I & (\mathcal{D}_{z12}+\mathcal{D}_{z11}R\mathcal{D}_y)^T \\ \star & \star & \star & \star & \star & \gamma_\infty^2 I \end{bmatrix} \succ \mathbf{0}. \tag{49}$$

Box I.

and Eq. (49) is given as in Box I. If a feasible solution set to the above inequalities exists, then the controller matrices can be obtained by using (36).

Proof. Since there are two different types of control constraints, we have to consider two different versions of the matrix inequality condition (34). First, setting the induced ℓ_∞ gain α to $\bar{u}_i/\|w\|_\infty$ and choosing $\mathcal{C}_z = \mathcal{C}_{z2}$, $\mathcal{D}_{z1} = \mathcal{D}_{21}$ and $\mathcal{D}_{z2} = \mathcal{D}_{22}$ gives (47). Then, setting the induced ℓ_∞ gain α to $\bar{v}_i/\|w\|_\infty$ and choosing $\mathcal{C}_z = \mathcal{C}_{z3}$, $\mathcal{D}_{z1} = \mathcal{D}_{31}$ and $\mathcal{D}_{z2} = \mathcal{D}_{32}$ yields (48). Note that existence of feasible solutions to these LMIs (47), (48) for all $i = 1, \ldots, m$ guarantee that the control signal never exceeds the magnitude and rate limits given in (2). Finally, setting $\mathcal{C}_z = \mathcal{C}_{z1}$, $\mathcal{D}_{z1} = \mathcal{D}_{z11}$, $\mathcal{D}_{z2} = \mathcal{D}_{z12}$ in (35) yields (49). Note that it follows from Theorem 1 that a feasible solution to (49) guarantees that $\|\mathbf{H}_{z_1,w}\|_{\ell_2 \leftarrow \ell_2} < \gamma_\infty$.

3.2. Robust induced ℓ_2/ℓ_∞ control

Consider the scenario when the original system (1) is uncertain and the unknown uncertainty matrix $\Delta(k)$ is time-varying. Then, following the similar notation in [6] one can define uncertainty on system matrices by using Linear Fractional Transformation (LFT) [49] as follows:

$$\begin{aligned} &\left[\mathcal{A}(\Delta(k)) \mid \mathcal{B}(\Delta(k)) \mid \mathcal{H}(\Delta(k))\right] \\ &= \left[\mathcal{A} \mid \mathcal{B} \mid \mathcal{H}\right] + \mathcal{B}_p\Delta(k)\left[I - \mathcal{D}_p\Delta(k)\right]^{-1}\left[\mathcal{A}_d \mid \mathcal{B}_d \mid \mathcal{H}_d\right], \end{aligned} \tag{50}$$

where $\mathcal{A}_d$, $\mathcal{B}_d$, $\mathcal{H}_d$, $\mathcal{B}_p$ and $\mathcal{D}_p$ are known system matrices of appropriate dimensions. Note that all uncertain matrices are assumed to be rationally dependent on $\Delta(k)$. For notational convenience, from this point onward, we shall drop time dependence k and denote $\Delta(k)$ with $\Delta \in \mathbf{\Delta}$, $\forall\, k \geq 0$ and $\mathbf{\Delta}$ is a bounded uncertainty set with known limits.

In this paper, we have opted to use full block S-procedure [45] to solve our problem as it has been already shown in the literature that this method provides less conservative LMI results. Our robust control approach to the issue described in Section 2 with uncertain system matrices supplied in (50), is based on the following lemma which requires the definition of the multiplier matrix Φ, and a parameter matrix $\bar{\Delta} \in \bar{\mathbf{\Delta}}$ that satisfy

$$\begin{bmatrix} \bar{\Delta}^T \\ I \end{bmatrix}^T \underbrace{\begin{bmatrix} \Psi & \chi \\ \chi^T & \Pi \end{bmatrix}}_{\Phi} \begin{bmatrix} \bar{\Delta}^T \\ I \end{bmatrix} = \bar{\Delta}\Psi\bar{\Delta}^T + \mathrm{He}\{\bar{\Delta}\chi\} + \Pi \preceq 0, \ \forall\, \bar{\Delta} \in \bar{\mathbf{\Delta}}. \tag{51}$$

Also, let us introduce the LFT

$$\bar{\Delta} \star \underbrace{\left[\begin{array}{c|c} \mathcal{Y}_{11} & \mathcal{Y}_{12} \\ \hline \mathcal{Y}_{21} & \mathcal{Y}_{22} \end{array}\right]}_{\mathcal{Y}} \triangleq \mathcal{Y}_{22} + \mathcal{Y}_{21}\bar{\Delta}(I - \mathcal{Y}_{11}\bar{\Delta})^{-1}\mathcal{Y}_{12}, \tag{52}$$

Note that the above LFT is called well-posed if $(I - \mathcal{Y}_{11}\bar{\Delta})$ is nonsingular for all $\bar{\Delta} \in \bar{\mathbf{\Delta}}$.

Lemma 2 ([50]).

$$\mathrm{He}\{\bar{\Delta} \star \mathcal{Y}\} \triangleq \bar{\Delta} \star \mathcal{Y} + (\bar{\Delta} \star \mathcal{Y})^T \succeq \mathbf{0}, \ \bar{\Delta} \in \bar{\mathbf{\Delta}}, \tag{53}$$

and the linear fractional transformation $\bar{\Delta} \star \mathcal{Y}$ is well-posed if and only if there exists a matrix Φ that satisfies (51) and

$$\begin{bmatrix} \mathcal{Y}_{21}\Pi\mathcal{Y}_{21}^T + \mathrm{He}\{\mathcal{Y}_{22}\} & \mathcal{Y}_{21}\Pi\mathcal{Y}_{11}^T + \mathcal{Y}_{21}\chi^T + \mathcal{Y}_{12}^T \\ * & \Psi + \mathcal{Y}_{11}\Pi\mathcal{Y}_{11}^T + \mathrm{He}\{\mathcal{Y}_{11}\chi^T\} \end{bmatrix} \succeq \mathbf{0}. \tag{54}$$

Now it is possible for us to establish the following results. In sequel, first, we will consider the case when full-state feedback information is available and then we will adapt the results of nominal output-feedback control solution to the systems having uncertain system matrices.

3.2.1. Robust state-feedback control

Theorem 5. *Consider uncertain system (1), which is subject to magnitude and rate bounds given in (2) and having uncertain system matrices of the form (50). Given the constants $\gamma_\infty > 0$ and $\lambda \in (0, 1)$, and based on the definition of augmented system matrices in (3), there exists a robust state-feedback type controller of the form (6) where $\mu(k) = K\underbrace{\left[x^T(k) \quad u^T(k-1) \quad v^T(k-1)\right]^T}_{\bar{x}^T(k)}$, which satisfies $\|\mathbf{H}_{z_1,w}\|_{\ell_2 \leftarrow \ell_2} < \gamma_\infty$ and the magnitude and rate constraints given in (2), if there exist a scalar $\rho > 0$, matrices $X = X^T \succ \mathbf{0}$, $W = W^T \succ \mathbf{0}$, $\Pi = \Pi^T$, $\Psi = \Psi^T$, χ, L and G which satisfy (26), (27), (51) along with*

$$\begin{bmatrix} G+G^T-X+\mathcal{B}_p\Pi\mathcal{B}_p^T & \mathcal{A}G+\mathcal{B}L & \mathcal{H} & \mathcal{B}_p\Pi\mathcal{D}_p^T+\mathcal{B}_p\chi^T \\ G^T\mathcal{A}^T+L^T\mathcal{B}^T & (1-\lambda)X & \mathbf{0} & G^T\mathcal{A}_d^T+L^T\mathcal{B}_d^T \\ \mathcal{H}^T & \mathbf{0} & \rho I & \mathcal{H}_d^T \\ \mathcal{D}_p\Pi\mathcal{B}_p^T+\chi\mathcal{B}_p^T & \mathcal{A}_dG+\mathcal{B}_dL & \mathcal{H}_d^T & \Psi+\mathcal{D}_p\Pi\mathcal{D}_p^T+\mathbf{He}\{\mathcal{D}_p\chi^T\} \end{bmatrix} \succ \mathbf{0}, \tag{55}$$

and

$$\begin{bmatrix} W+\mathcal{B}_p\Pi\mathcal{B}_p^T & \mathcal{A}G+\mathcal{B}L & \mathcal{H} & \mathbf{0} & \mathcal{B}_p\Pi\mathcal{D}_p^T+\mathcal{B}_p\chi^T \\ \star & G+G^T-W & \mathbf{0} & G^T\mathcal{C}_{z1}^T+L^T\mathcal{D}_{z11}^T & G^T\mathcal{A}_d^T+L^T\mathcal{B}_d^T \\ \star & \star & I & \mathcal{D}_{z12}^T & \mathcal{H}_d^T \\ \star & \star & \star & \gamma_\infty^2 I & \mathbf{0} \\ \star & \star & \star & \star & \Psi+\mathcal{D}_p\Pi\mathcal{D}_p^T+\mathbf{He}\{\mathcal{D}_p\chi^T\} \end{bmatrix} \succ \mathbf{0}, \tag{56}$$

for all $i = 1, \ldots, m$.

If a feasible set of solution is obtained to this problem, then the feedback control gain can be obtained as $K = LG^{-1}$.

Proof. We will consider only the LMIs which involve uncertain system matrices in Theorem 2. In the light of the definitions of uncertain system matrices (50), matrix inequality (25) can be

expanded as

$$\underbrace{\begin{bmatrix} G+G^T-X & \mathcal{A}G+\mathcal{B}L & \mathcal{H} \\ \star & (1-\lambda)X & \mathbf{0} \\ \star & \star & \rho I \end{bmatrix}}_{\mathcal{Y}_{22}^T+\mathcal{Y}_{22}} + \mathbf{He}\left\{ \underbrace{\begin{bmatrix} \mathcal{B}_p \\ \mathbf{0} \\ \mathbf{0} \end{bmatrix}}_{\mathcal{Y}_{21}} \underbrace{\Delta}_{\bar{\Delta}} (I - \underbrace{\mathcal{D}_p}_{\mathcal{Y}_{11}} \Delta)^{-1} \underbrace{\begin{bmatrix} \mathbf{0} & \mathcal{A}_d G + \mathcal{B}_d L & \mathcal{H}_d \end{bmatrix}}_{\mathcal{Y}_{12}} \right\} \succ \mathbf{0}. \quad (57)$$

Hence, if we apply Lemma 2 on (57) by utilising the definition of $\mathcal{Y}$, one can obtain (55). Similarly, based on the uncertain system matrix definitions (50), (28) can be written as

$$\underbrace{\begin{bmatrix} W & \mathcal{A}G+\mathcal{B}L & \mathcal{H} & \mathbf{0} \\ \star & G+G^T-W & \mathbf{0} & G^T\mathcal{C}_{z1}^T + L^T\mathcal{D}_{z11}^T \\ \star & \star & I & \mathcal{D}_{z12}^T \\ \star & \star & \star & \gamma_\infty^2 I \end{bmatrix}}_{\mathcal{Y}_{22}+\mathcal{Y}_{22}^T} + \mathbf{He}\left\{ \underbrace{\begin{bmatrix} \mathcal{B}_p \\ \mathbf{0} \\ \mathbf{0} \\ \mathbf{0} \end{bmatrix}}_{\mathcal{Y}_{21}} \underbrace{\Delta}_{\bar{\Delta}} (I - \underbrace{\mathcal{D}_p}_{\mathcal{Y}_{11}} \Delta)^{-1} \underbrace{\begin{bmatrix} \mathbf{0} & \mathcal{A}_d G + \mathcal{B}_d L & \mathcal{H}_d & \mathbf{0} \end{bmatrix}}_{\mathcal{Y}_{12}} \right\} \succ \mathbf{0}. \quad (58)$$

Then, application of Lemma 2 on (58) gives (56). This concludes the proof.

3.2.2. Robust output-feedback control

The following theorem describes a methodological design approach for a robust dynamic output-feedback controller that solves the challenge presented in Section 2.

Theorem 6. *Consider system (1) which is subject to magnitude and rate bounds given in (2) and having uncertain system matrices of the form (50). Given the constants $\gamma_\infty > 0$ and $\lambda \in (0,1)$, and based on the definition of augmented system matrices in (3), there exists a robust dynamic output-feedback controller of the form (6) with*

$$\begin{aligned} x_c(k+1) &= \mathcal{A}_c x_c(k) + \mathcal{B}_c \bar{y}(k) \\ \mu(k) &= \mathcal{C}_c x_c(k) + \mathcal{D}_c \bar{y}(k) \end{aligned} \quad (59)$$

that satisfies $\|\mathcal{T}_{z_1,w}\|_{\ell_2\to\ell_2} < \gamma_\infty$ and the magnitude and rate constraints given in (2), if there exist $\rho > 0$ and matrices G_{11}, $\mathsf{X} = \mathsf{X}^T \succ \mathbf{0}$, $M = M^T \succ \mathbf{0}$, $\mathsf{W} = \mathsf{W}^T \succ \mathbf{0}$, $E = E^T \succ \mathbf{0}$, J, S, R, N, F, Y, Z, Q and $\Pi = \begin{bmatrix} \Pi_{11} & \Pi_{12} \\ \Pi_{12}^T & \Pi_{22} \end{bmatrix}$, $\Psi = \begin{bmatrix} \Psi_{11} & \Psi_{12} \\ \Psi_{12}^T & \Psi_{22} \end{bmatrix}$, $\chi = \begin{bmatrix} \chi_{11} & \chi_{12} \\ \chi_{21} & \chi_{22} \end{bmatrix}$, which satisfy the LMIs, (47), (48) and (51) for all $i = 1, \ldots, m$, along with

$$\begin{bmatrix} \Sigma_{11} & I+S^T-J & \mathcal{A}G_{11}+\mathcal{B}N & \Sigma_{14} & \Sigma_{15} \\ \star & Y+Y^T-M & Q & Y\mathcal{A}+F\mathcal{C}_y & Y\mathcal{H}+F\mathcal{D}_y \\ \star & \star & (1-\lambda)\mathsf{X} & (1-\lambda)J & \mathbf{0} \\ \star & \star & \star & \Sigma_{44} & \mathcal{A}_d^T\Pi_{22}\mathcal{H}_d \\ \star & \star & \star & \star & \rho I + \mathcal{H}_d^T\Pi_{22}\mathcal{H}_d \\ \star & \star & \star & \star & \star \\ \star & \star & \star & \star & \star \end{bmatrix}$$
$$\begin{bmatrix} \mathcal{B}_p\Pi_{11}\mathcal{D}_p^T + \mathcal{B}_p\chi_{11}^T & \mathcal{B}_p\Pi_{12}\mathcal{D}_p + \mathcal{B}_p\chi_{21}^T \\ \mathbf{0} & Y\mathcal{B}_p \\ G_{11}^T\mathcal{A}_d^T + N^T\mathcal{B}_d^T & \mathbf{0} \\ \Sigma_{46} & \mathcal{A}_d^T\Pi_{22}\mathcal{D}_p + \mathcal{A}_d^T\chi_{22}^T \\ \Sigma_{56} & \mathcal{H}_d^T\chi_{22}^T + \mathcal{H}_d^T\Pi_{22}\mathcal{D}_p \\ \Sigma_{66} & \Sigma_{67} \\ \star & \Sigma_{77} \end{bmatrix} \succ \mathbf{0}, \quad (60)$$

where

$$\begin{aligned} \Sigma_{11} &= G_{11}^T + G_{11} - \mathsf{X} + \mathcal{B}_p\Pi_{11}\mathcal{B}_p^T, \\ \Sigma_{14} &= \mathcal{A} + \mathcal{B}R\mathcal{C}_y + \mathcal{B}_p\Pi_{12}\mathcal{A}_d, \ \Sigma_{15} = \mathcal{H} + \mathcal{B}R\mathcal{D}_y + \mathcal{B}_p\Pi_{12}\mathcal{H}_d, \\ \Sigma_{44} &= (1-\lambda)M + \mathcal{A}_d^T\Pi_{22}\mathcal{A}_d^T, \\ \Sigma_{46} &= \mathcal{A}_d^T\Pi_{12}^T\mathcal{D}_p^T + \mathcal{A}_d^T\chi_{12}^T + \mathcal{A}_d^T + \mathcal{C}_y^T R^T \mathcal{B}_d^T, \\ \Sigma_{56} &= \mathcal{H}_d^T\Pi_{12}^T\mathcal{D}_p^T + \mathcal{H}_d^T\chi_{12}^T + \mathcal{H}_d^T + \mathcal{D}_y^T R^T \mathcal{B}_d^T, \\ \Sigma_{66} &= \Psi_{11} + \mathcal{D}_p\Pi_{11}\mathcal{D}_p^T + \mathcal{D}_p\chi_{11}^T + \chi_{11}\mathcal{D}_p^T, \\ \Sigma_{67} &= \Psi_{12} + \mathcal{D}_p\Pi_{12}\mathcal{D}_p + \mathcal{D}_p\chi_{12} + \chi_{12}\mathcal{D}_p, \\ \Sigma_{77} &= \Psi_{22} + \mathcal{D}_p^T\Pi_{22}\mathcal{D}_p + \mathcal{D}_p^T\chi_{22}^T + \chi_{22}\mathcal{D}_p, \end{aligned}$$

and

$$\begin{bmatrix} \mathsf{W}+\mathcal{B}_p\Pi_{11}\mathcal{B}_p^T & Z & \mathcal{A}G_{11}+\mathcal{B}N & \Gamma_{14} & \Gamma_{15} \\ \star & E & Q & Y\mathcal{A}+F\mathcal{C}_y & Y\mathcal{H}+F\mathcal{D}_{y2} \\ \star & \star & G_{11}+G_{11}^T-\mathsf{W} & I+S^T-Z & \mathbf{0} \\ \star & \star & \star & \Gamma_{44} & \mathcal{A}_d^T\Pi_{22}\mathcal{H}_d \\ \star & \star & \star & \star & I+\mathcal{H}_d^T\Pi_{22}\mathcal{H}_d \\ \star & \star & \star & \star & \star \\ \star & \star & \star & \star & \star \\ \star & \star & \star & \star & \star \end{bmatrix}$$
$$\begin{bmatrix} \mathbf{0} & \mathcal{B}_p\Pi_{11}\mathcal{D}_p^T + \mathcal{B}_p\chi_{11}^T & \Gamma_{18} \\ \mathbf{0} & \mathbf{0} & Y\mathcal{B}_p \\ (\mathcal{C}_{z1}G_{11}+\mathcal{D}_{z11}N)^T & G_{11}^T\mathcal{A}_d^T + N^T\mathcal{B}_d^T & \mathbf{0} \\ (\mathcal{C}_{z1}+\mathcal{D}_{z11}R\mathcal{C}_y)^T & \Gamma_{47} & \Gamma_{48} \\ (\mathcal{D}_{z12}+\mathcal{D}_{z11}R\mathcal{D}_{y2})^T & \Gamma_{57} & \Gamma_{58} \\ \gamma_\infty^2 I & \mathbf{0} & \mathbf{0} \\ \star & \Gamma_{77} & \Gamma_{78} \\ \star & \star & \Gamma_{88} \end{bmatrix} \succ \mathbf{0}, \quad (61)$$

where

$$\begin{aligned} \Gamma_{14} &= \mathcal{A} + \mathcal{B}R\mathcal{C}_y + \mathcal{B}_p\Pi_{12}\mathcal{A}_d, \ \Gamma_{15} = \mathcal{H} + \mathcal{B}R\mathcal{D}_y + \mathcal{B}_p\Pi_{12}\mathcal{H}_d, \\ \Gamma_{18} &= \mathcal{B}_p\Pi_{12}\mathcal{D}_p + \mathcal{B}_p\chi_{21}^T, \ \Gamma_{44} = Y + Y^T - E + \mathcal{A}_d^T\Pi_{22}\mathcal{A}_d, \\ \Gamma_{47} &= \mathcal{A}_d^T\chi_{12}^T + \mathcal{A}_d^T\Pi_{12}^T\mathcal{D}_p^T + \mathcal{A}_d^T + \mathcal{C}_y^T R^T \mathcal{B}_d^T, \\ \Gamma_{48} &= \mathcal{A}_d^T\Pi_{22}\mathcal{D}_p + \mathcal{A}_d^T\chi_{22}^T, \\ \Gamma_{57} &= \mathcal{H}_d^T\chi_{12}^T + \mathcal{H}_d^T\Pi_{12}^T\mathcal{D}_p^T + \mathcal{H}_d^T + \mathcal{D}_y^T R^T \mathcal{B}_d^T, \\ \Gamma_{58} &= \mathcal{H}_d^T\chi_{22}^T + \mathcal{H}_d^T\Pi_{22}\mathcal{D}_p, \\ \Gamma_{77} &= \Psi_{11} + \mathcal{D}_p\Pi_{11}\mathcal{D}_p^T + \mathcal{D}_p\chi_{11}^T + \chi_{11}\mathcal{D}_p^T, \\ \Gamma_{78} &= \Psi_{12} + \mathcal{D}_p\Pi_{12}\mathcal{D}_p + \mathcal{D}_p\chi_{12} + \chi_{12}\mathcal{D}_p \text{ and} \\ \Gamma_{88} &= \Psi_{22} + \mathcal{D}_p^T\Pi_{22}\mathcal{D}_p + \mathcal{D}_p^T\chi_{22}^T + \chi_{22}\mathcal{D}_p. \end{aligned}$$

If a feasible set of solution to the above inequalities exists, then the controller matrices can be obtained by using Eq. (36).

Proof. The only changes in Corollary 4 will be on the matrix inequality conditions which involve uncertain system matrices $\mathcal{A}$, $\mathcal{B}$ and $\mathcal{H}$. Using the uncertain matrix definitions (50), and the appropriate matrix partitioning $\Pi \triangleq \begin{bmatrix} \Pi_{11} & \Pi_{12} \\ \Pi_{12}^T & \Pi_{22} \end{bmatrix}$, $\Psi \triangleq \begin{bmatrix} \Psi_{11} & \Psi_{12} \\ \Psi_{12}^T & \Psi_{22} \end{bmatrix}$ and $\chi \triangleq \begin{bmatrix} \chi_{11} & \chi_{12} \\ \chi_{21} & \chi_{22} \end{bmatrix}$, the LMI condition (33) can be written and partitioned as follows:

$$\underbrace{\begin{bmatrix} G_{11}+G_{11}^T-\mathsf{X} & I+S^T-J & \mathcal{A}G_{11}+\mathcal{B}N & \mathcal{A}+\mathcal{B}R\mathcal{C}_y & \mathcal{H}+\mathcal{B}R\mathcal{D}_y \\ \star & Y+Y^T-M & Q & Y\mathcal{A}+F\mathcal{C}_y & Y\mathcal{H}+F\mathcal{D}_y \\ \star & \star & (1-\lambda)\mathsf{X} & (1-\lambda)J & \mathbf{0} \\ \star & \star & \star & (1-\lambda)M & \mathbf{0} \\ \star & \star & \star & \star & \rho I \end{bmatrix}}_{\mathcal{Y}_{22}^T+\mathcal{Y}_{22}}$$

$$+\mathbf{He}\left\{\underbrace{\begin{bmatrix}\mathcal{B}_p & \mathbf{0}\\ \mathbf{0} & \mathbf{0}\\ \mathbf{0} & \mathbf{0}\\ \mathbf{0} & \mathcal{A}_d^T\\ \mathbf{0} & \mathcal{H}_d^T\end{bmatrix}}_{\mathcal{Y}_{21}}\underbrace{\begin{bmatrix}\Delta & \mathbf{0}\\ \mathbf{0} & \Delta^T\end{bmatrix}}_{\bar{\Delta}}\left[\begin{bmatrix}I & \mathbf{0}\\ \mathbf{0} & I\end{bmatrix}-\underbrace{\begin{bmatrix}\mathcal{D}_p & \mathbf{0}\\ \mathbf{0} & \mathcal{D}_p^T\end{bmatrix}}_{\mathcal{Y}_{11}}\begin{bmatrix}\Delta & \mathbf{0}\\ \mathbf{0} & \Delta^T\end{bmatrix}\right]^{-1}\right.$$

$$\left.\times\underbrace{\begin{bmatrix}\mathbf{0} & \mathbf{0} & \mathcal{A}_dG_{11}+\mathcal{B}_dN & \mathcal{A}_d+\mathcal{B}_dR\mathcal{C}_y & \mathcal{H}_d+\mathcal{B}_dR\mathcal{D}_y\\ \mathbf{0} & \mathcal{B}_p^TY^T & \mathbf{0} & \mathbf{0} & \mathbf{0}\end{bmatrix}}_{\mathcal{Y}_{12}}\right\}\succ 0. \quad (62)$$

Then, application of the LMI condition (54) using the under-braced matrix definitions shown above, leads to (60).

Similarly, based on the uncertain matrix definitions (50), matrix inequality (49) can be written as

$$\underbrace{\begin{bmatrix}\mathsf{W} & Z & \mathcal{A}G_{11}+\mathcal{B}N & \mathcal{A}+\mathcal{B}R\mathcal{C}_y & \mathcal{H}+\mathcal{B}R\mathcal{D}_y & \mathbf{0}\\ \star & E & Q & Y\mathcal{A}+F\mathcal{C}_y & Y\mathcal{H}+F\mathcal{D}_y & \mathbf{0}\\ \star & \star & G_{11}+G_{11}^T-\mathsf{W} & I+S^T-Z & \mathbf{0} & (\mathcal{C}_{z1}G_{11}+\mathcal{D}_{z11}N)^T\\ \star & \star & \star & Y+Y^T-E & \mathbf{0} & (\mathcal{C}_{z1}+\mathcal{D}_{z11}R\mathcal{C}_y)^T\\ \star & \star & \star & \star & I & (\mathcal{D}_{z12}+\mathcal{D}_{z11}R\mathcal{D}_y)^T\\ \star & \star & \star & \star & \star & \gamma_\infty^2 I\end{bmatrix}}_{\mathcal{Y}_{22}^T+\mathcal{Y}_{22}}$$

$$+\mathbf{He}\left\{\underbrace{\begin{bmatrix}\mathcal{B}_p & \mathbf{0}\\ \mathbf{0} & \mathbf{0}\\ \mathbf{0} & \mathbf{0}\\ \mathbf{0} & \mathcal{A}_d^T\\ \mathbf{0} & \mathcal{H}_d^T\\ \mathbf{0} & \mathbf{0}\end{bmatrix}}_{\mathcal{Y}_{21}}\underbrace{\begin{bmatrix}\Delta & \mathbf{0}\\ \mathbf{0} & \Delta^T\end{bmatrix}}_{\bar{\Delta}}\left[\begin{bmatrix}I & \mathbf{0}\\ \mathbf{0} & I\end{bmatrix}-\underbrace{\begin{bmatrix}\mathcal{D}_p & \mathbf{0}\\ \mathbf{0} & \mathcal{D}_p^T\end{bmatrix}}_{\mathcal{Y}_{11}}\begin{bmatrix}\Delta & \mathbf{0}\\ \mathbf{0} & \Delta^T\end{bmatrix}\right]^{-1}\right.$$

$$\left.\times\underbrace{\begin{bmatrix}\mathbf{0} & \mathbf{0} & \mathcal{A}_dG_{11}+\mathcal{B}_dN & \mathcal{A}_d+\mathcal{B}_dR\mathcal{C}_y & \mathcal{H}_d+\mathcal{B}_dR\mathcal{D}_y & \mathbf{0}\\ \mathbf{0} & \mathcal{B}_p^TY^T & \mathbf{0} & \mathbf{0} & \mathbf{0} & \mathbf{0}\end{bmatrix}}_{\mathcal{Y}_{12}}\right\}\succ 0, \quad (63)$$

which is equivalent to (61), according to the matrix definitions and Lemma 2. This concludes the proof.

We stress that for all admissible values of $\bar{\Delta}\in\bar{\mathbf{\Delta}}$, (51) needs to be satisfied. However, this requires the feasibility of infinite number of LMI conditions, which is practically impossible to satisfy. Therefore, tractable sufficient conditions are needed to replace (53). As a solution to this intermediate problem, we employ LMI relaxations that ensure the satisfaction of (51). In general, for polytopic regions, convex-hull relaxation or P'olya's approach can be used. If the regions can be characterised by polynomial inequalities, the sum-of-squares (SOS) method might be more appropriate [51,52]. For the feasibility of (51), in this study, we used Pólya type relaxations [53]. One can refer to Section 5.1.2 of the paper [6] for the details and application of the approach.

Remark 2. Although, different multiplier matrix Φ could be used for each matrix inequality having uncertain entries in Theorem 2 and Corollary 4, in this paper, we opted to use common uncertainty multiplier matrix Φ to reduce computational load.

4. Simulation study

We shall consider two different examples to show the effectiveness and application of the proposed methods of this paper. During simulations studies, we have used MATLAB, with the parser YALMIP [54] and the semi-definite optimisation solvers SeDuMi and Mosek.

Example 1. We consider the example of pitch rate control of an aircraft that is also studied in [36] as a benchmark problem. The aircraft transfer function $G_p(s)$, which has the pitch rate $\dot{\theta}$, as the output, and the elevator deflection, as the input, u, is given by

$$G_p(s)=\frac{\dot{\theta}(s)}{U(s)}=\frac{-10(s+1)(s+0.01)}{(s^2+2s+2)(s^2+0.02s+0.0101)}. \quad (64)$$

The problem we consider is to control the rate of pitch angle to track a given reference command signal r as close as possible. Following [36], the control input is subject to hard magnitude and rate constraints as follows: $\bar{u}=6$ [deg], $\bar{v}=10$ [deg/s].

Before we proceed with the application of the proposed method, the disturbance rejection problem needs to be translated into a reference tracking problem. To this end, let us define an accumulated tracking-error signal $e(k)=r(k)-T\tilde{y}(k)+e(k-1)$ where $e(-1)=0$. Here, $T\tilde{y}(k)$ is the manipulated output with a known matrix T in appropriate dimension. In this problem, $T=1$ since we have a single controlled output $\dot{\theta}$, which is identical to the measured feedback signal. Then the servo-mechanism system can be defined in state-space as follows:

$$x(k+1)=\underbrace{\begin{bmatrix}I & -T\tilde{C}_y\\ \mathbf{0} & \tilde{A}\end{bmatrix}}_{A}x(k)+\underbrace{\begin{bmatrix}\mathbf{0}\\ \tilde{B}\end{bmatrix}}_{B}u(k)+\underbrace{\begin{bmatrix}I\\ \mathbf{0}\end{bmatrix}}_{H}r(k),$$

$$z_1(k)=\underbrace{\begin{bmatrix}W_1 & -W_2T\tilde{C}_y\end{bmatrix}}_{C_{z1}}\underbrace{\begin{bmatrix}e(k-1)\\ \tilde{x}(k)\end{bmatrix}}_{x(k)}+\underbrace{\begin{bmatrix}\mathbf{0}\end{bmatrix}}_{D_{z1}}u(k)+\underbrace{\begin{bmatrix}W_2\end{bmatrix}}_{D_{z2}}r(k),$$

$$y(k)=\underbrace{\begin{bmatrix}I & \mathbf{0}\\ \mathbf{0} & \mathbf{0}\\ \mathbf{0} & \tilde{C}_y\end{bmatrix}}_{C_y}x(k)+\underbrace{\begin{bmatrix}\mathbf{0}\\ I\\ \mathbf{0}\end{bmatrix}}_{D_{y2}}r(k). \quad (65)$$

Discretising the system transfer function (64) with a sampler having a sampling period $T_s=0.05$ s, gives

$$\tilde{x}(k+1)=\underbrace{\begin{bmatrix}0.9990 & -0.0050 & -0.0019 & -0.0000\\ 0.0050 & 1.0000 & -0.0001 & -0.0000\\ 0.0019 & -0.0001 & 0.9026 & 0.0672\\ -0.0000 & 0.0000 & -0.0672 & 0.9975\end{bmatrix}}_{\tilde{A}}\tilde{x}(k)+\underbrace{\begin{bmatrix}-0.1122\\ 0.0055\\ 0.1065\\ -0.0008\end{bmatrix}}_{\tilde{B}}u(k)$$

$$\tilde{y}(k)=\underbrace{\begin{bmatrix}2.2425 & 0.1153 & 2.2404 & -0.0611\end{bmatrix}}_{\tilde{C}_y}\tilde{x}(k) \quad (66)$$

Here, we take $\tilde{y}(k)=\tilde{\dot{\theta}}(k)$ and without loss of generality, we assume that the controller can access to the information of the tracking error at the previous sample, $e(k-1)$, and the reference signal $r(k)$ for all $k\geq 0$. On the other hand, we used the filtered accumulated tracking error as the controlled output with diagonal weighting matrices W_1 and W_2 whose values are to be selected by the designer depending on the transient performance of the system. In this example, reasonable transient response is achieved with the selections of $W_1=16$ and $W_2=20$. The extended state vector is chosen as $\bar{x}^T=\begin{bmatrix}e(k-1) & \tilde{x}^T(k) & u(k-1) & v(k-1)\end{bmatrix}$. Then, according to this selection, $w(k)=r(k)$ with $\|w\|_\infty=1$, $\mathcal{C}_{z1}=\begin{bmatrix}C_z & 0 & 0\end{bmatrix}$ where $C_z=\begin{bmatrix}16 & -20\tilde{C}_y\end{bmatrix}$, $\mathcal{D}_{z11}=\begin{bmatrix}0\end{bmatrix}$, $\mathcal{D}_{z12}=20$, $\mathcal{C}_{z2}=\begin{bmatrix}0 & 0 & 0 & 0 & 0 & 1 & 1\end{bmatrix}$, $\mathcal{C}_{z3}=\begin{bmatrix}0 & 0 & 0 & 0 & 0 & 0 & 1\end{bmatrix}$,

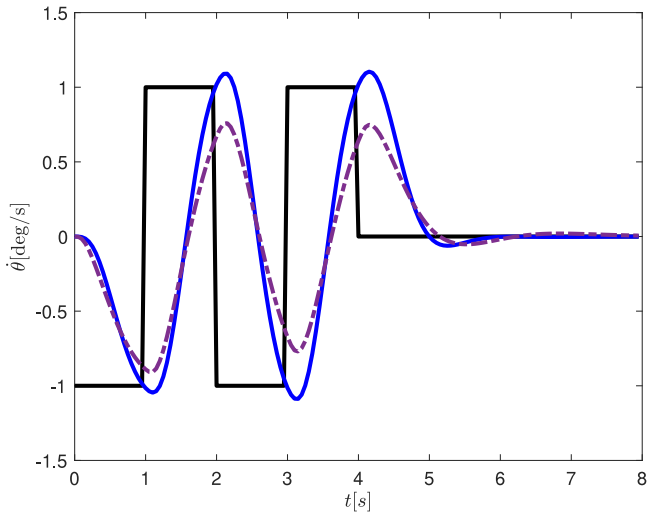

Fig. 1. Variation of the rate of pitch angle $\dot{\theta}(t)$ when $\bar{u} = 6$ [deg] and $\bar{v} = 10$ [deg/s]. The reference signal, r is denoted by solid black line. Solid blue trajectory demonstrates the output of the system when the system is controlled with the proposed controller. Dot-dashed lines shows the performance of the multi-stage AW controller proposed by [36].

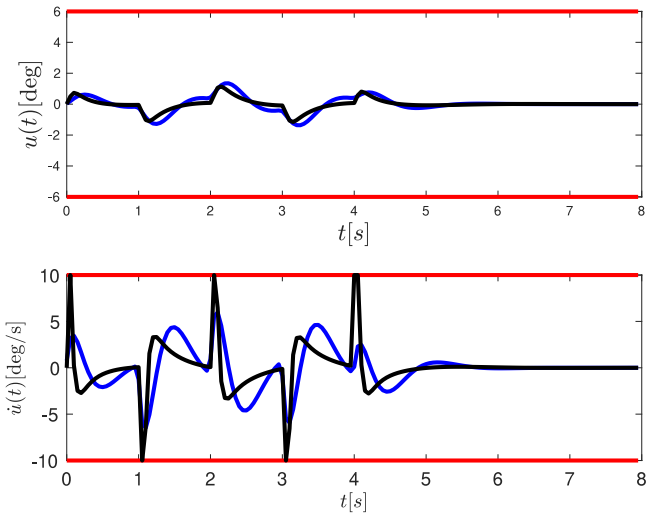

Fig. 2. Control signal, $u(t)$ and its rate $\dot{u}(t)$ for the proposed controller (blue) and the multi stage AW controller (black).

$\mathcal{D}_{z21} = \mathcal{D}_{z31} = 1$, $\mathcal{D}_{z31} = 1$, $\mathcal{D}_{z32} = 0$. In order to find the optimum value of λ, a line search is performed. To this end, the line segment, $(0, 1)$ is divided into 100 equidistant points with a resolution of 0.01 and all feasible values of γ_∞ are recorded for each value of λ. We achieve the minimum value $\gamma_\infty = 178$ for $\lambda = 0.11$. Fig. 1 shows the tracking response of the proposed controller in comparison with those of the multi-stage AW controller proposed in [36]. For a fair comparison, we used the controller and its settings presented in [36].

Fig. 2, on the other hand, depicts the variance of these controllers' control and rate-of-control signals. From the figures, one can easily conclude that the proposed output-feedback controller demonstrates better performance than those of a multi-stage AW controller using similar amount of control energy. Also, at this point, it is worth mentioning that the proposed controller of this paper can still demonstrate a reasonably acceptable performance even when the MRBs are reduced to $\bar{u} = 4$ [deg] and $\bar{v} = 7$ [deg/s], which is not possible by using the method of [36]. Fig. 3 shows the variation of the rate of the pitch angle, $\dot{\theta}(t)$ with respect to the same reference signal used in the previous simulation and Fig. 4 shows the variation of the control signals.

Example 2. We consider the lateral–directional motion control problem of the F-4 fighter aircraft [55], a 2-input, 2-output (TITO) system with a state vector $x_{cont}(t) = \begin{bmatrix} p & \zeta & \beta & \phi & \varrho_r & \varrho_a \end{bmatrix}^T$, where p[rad/s] is the roll rate, ζ[rad/s] is the yaw rate, β[rad] is the side-slip angle, ϕ[rad] is the roll angle, ϱ_r[rad] is the applied rudder angle and ϱ_a[rad] is the applied aileron angle. The control input vector is $u_{cont}(t) = \begin{bmatrix} u_1 & u_2 \end{bmatrix}^T$, where u_1 and u_2 are command angles to the actuators of rudder and aileron in [rad], respectively. The output is $y_{cont} = \begin{bmatrix} \beta & \phi \end{bmatrix}^T$. Then, the system dynamics in CT state-space form can be represented as

$$\dot{x}_{cont}(t) = \begin{bmatrix} -0.764 & 0.387 & -12.9 & 0 & 0.952 & 6.05 \\ 0.024 & -0.174 & 4.31 & 0 & -1.76 & -0.416 \\ 0.006 & -0.999 & -0.0578 & 0.0369 & 0.0092 & -0.0012 \\ 1 & 0 & 0 & 0 & 0 & 0 \\ 0 & 0 & 0 & 0 & -10 & 0 \\ 0 & 0 & 0 & 0 & 0 & -5 \end{bmatrix} x_{cont}(t)$$

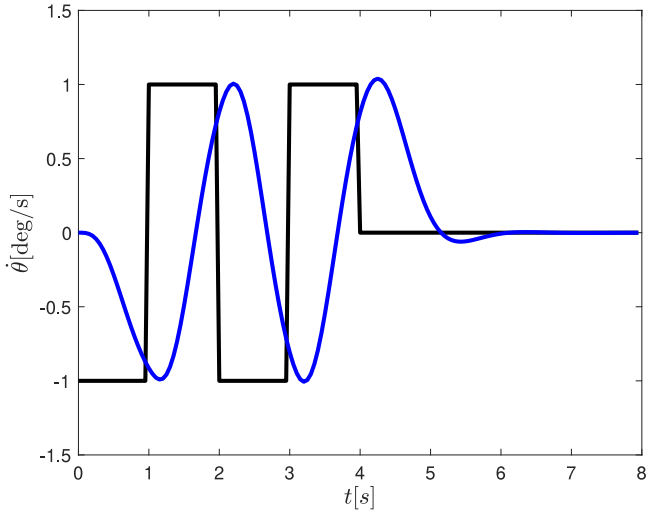

Fig. 3. Variation of the rate of pitch angle $\dot{\theta}(t)$ when the actuator bounds are reduced to $\bar{u} = 4$ [deg] and $\bar{v} = 7$ [deg/s]. The reference signal, r is denoted by solid black line. Solid blue trajectory demonstrates the output of the system when the system is controlled with the proposed controller.

$$+ \begin{bmatrix} 0 & 0 \\ 0 & 0 \\ 0 & 0 \\ 0 & 0 \\ 20 & 0 \\ 0 & 10 \end{bmatrix} u_{cont}(t), \tag{67}$$

$$y_{cont}(t) = \begin{bmatrix} 0 & 0 & 1 & 0 & 0 & 0 \\ 0 & 0 & 0 & 1 & 0 & 0 \end{bmatrix} x_{cont}(t).$$

Discretisation of the continuous-time process (67) using Tustin method with a sampling period $T_s = 0.5$ s yields

$$\tilde{A} = \begin{bmatrix} 0.6740 & 1.3676 & -4.1392 & -0.0463 & -0.1089 & 0.7915 \\ 0.0130 & 0.4646 & 1.6521 & 0.0173 & -0.1049 & -0.0431 \\ 0.0034 & -0.3894 & 0.4932 & 0.0151 & 0.0592 & 0.0247 \\ 0.4141 & 0.2624 & -1.2543 & 0.9917 & 0.0030 & 0.3213 \\ 0 & 0 & 0 & 0 & 0.0067 & 0 \\ 0 & 0 & 0 & 0 & 0 & 0.0821 \end{bmatrix}$$

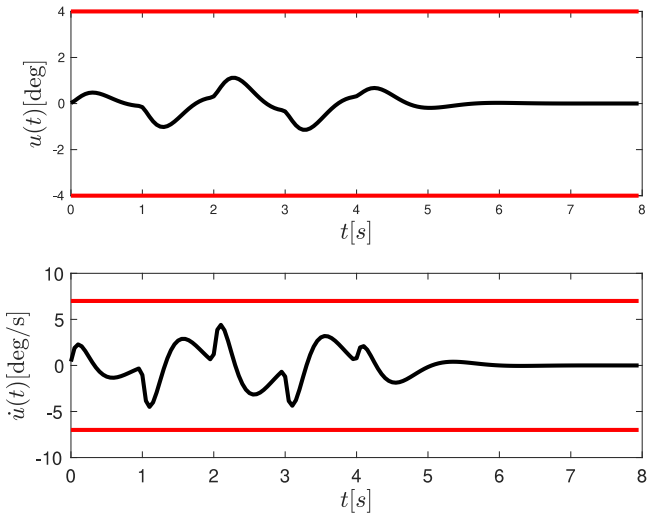

Fig. 4. Control signal, $u(t)$ and its rate $\dot{u}(t)$ for the proposed controller when the actuator limits are reduced to $\bar{u} = 4$ [deg] and $\bar{v} = 7$ [deg/s].

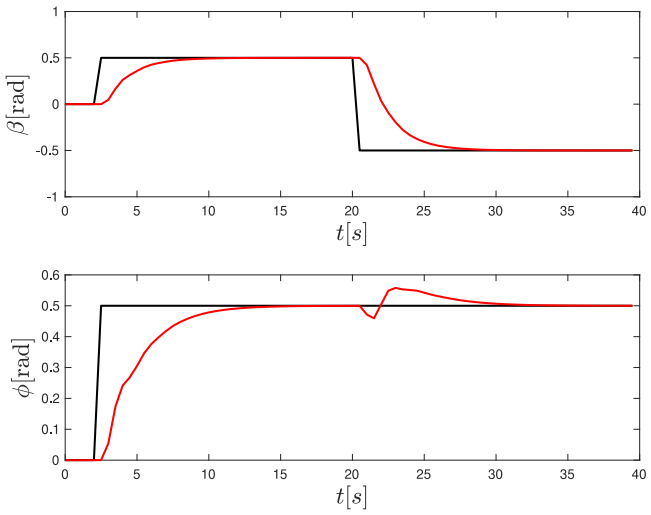

Fig. 5. (Nominal model, Example 2) Variation of the side-slip angle β (top-red) and roll angle ϕ (bottom-red) with respect to reference trajectories r_β (top-black) and r_ϕ (bottom-black) when the system is controlled by the proposed output-feedback control. (For interpretation of the references to colour in this figure legend, the reader is referred to the web version of this article.)

$$\tilde{B} = \begin{bmatrix} 0.0596 & 3.2129 \\ -1.1801 & -0.2088 \\ 0.2764 & 0.0509 \\ 0.0727 & 0.6627 \\ 1.9865 & 0 \\ 0 & 1.8358 \end{bmatrix}, \ \tilde{C}_y = \begin{bmatrix} 0 & 0 & 1 & 0 & 0 & 0 \\ 0 & 0 & 0 & 1 & 0 & 0 \end{bmatrix}. \tag{68}$$

Different from the paper [55], in this study, we assume that both control inputs are subject to magnitude and rate saturations as follows: $\bar{u}_1 = 0.7854$ [rad], $\bar{u}_2 = 0.5236$ [rad], $\bar{v}_1 = 1.3090$ [rad/s] and $\bar{v}_2 = 1.1345$ [rad/s]. The control task is to ensure that the outputs follow the following reference trajectories of the side-slip and roll angles with minimum error:

$$r_\beta(t) = \begin{cases} 0.5 & 3 \le t < 21 \\ -0.5 & 21 \le t \le 40, \\ 0 & \text{otherwise} \end{cases} \quad r_\phi(t) = \begin{cases} 0.5 & 3 \le t \le 40 \\ 0 & \text{otherwise} \end{cases} \tag{69}$$

We constitute the servo-mechanism augmentation defined in (65) by selecting $T = I$, $W_1 = 0.3 \times \text{diag}\{1/20, 1/20\}$, $W_2 = 0.7 \times \text{diag}\{1/20, 1/10\}$, $\mathcal{C}_{z1} = \begin{bmatrix} C_z & 0 & 0 & 0 & 0 \end{bmatrix}$ where $C_z = \begin{bmatrix} W_1 & -W_2 T \tilde{C}_y \end{bmatrix}$, $\mathcal{D}_{z11} = \mathbf{0}$, $\mathcal{D}_{z12} = W_2$, $\mathcal{C}^1_{z2} = \begin{bmatrix} 0 & 0 & 0 & 0 & 0 & 0 & 0 & 1 & 0 & 1 & 0 \end{bmatrix}$, $\mathcal{C}^2_{z2} = \begin{bmatrix} 0 & 0 & 0 & 0 & 0 & 0 & 0 & 0 & 1 & 0 & 1 \end{bmatrix}$, $\mathcal{C}^1_{z3} = \begin{bmatrix} 0 & 0 & 0 & 0 & 0 & 0 & 0 & 0 & 0 & 1 & 0 \end{bmatrix}$, $\mathcal{C}^2_{z3} = \begin{bmatrix} 0 & 0 & 0 & 0 & 0 & 0 & 0 & 0 & 0 & 0 & 1 \end{bmatrix}$, $\mathcal{D}^1_{z21} = \begin{bmatrix} 1 & 0 \end{bmatrix}$, $\mathcal{D}^2_{z21} = \begin{bmatrix} 0 & 1 \end{bmatrix}$, $\mathcal{D}^1_{z22} = \mathcal{D}^2_{z22} = \begin{bmatrix} 0 & 0 \end{bmatrix}$, $\mathcal{D}^1_{z31} = \begin{bmatrix} 1 & 0 \end{bmatrix}$, $\mathcal{D}^2_{z31} = \begin{bmatrix} 0 & 1 \end{bmatrix}$, $\mathcal{D}^1_{z32} = \mathcal{D}^2_{z32} = \begin{bmatrix} 0 & 0 \end{bmatrix}$ and $w(k) = r(k)$ where $r(k) = \begin{bmatrix} r_\beta(k) & r_\phi(k) \end{bmatrix}^T$. From (69), we infer that $\|w\|_\infty = 0.5$. Then, application of the proposed controller design approach yields the minimum achievable gain $\gamma_\infty = 0.078$ at $\lambda = 0.2507$. Note that, in this example, the measurement vector is chosen as $\bar{y}^T(k) = \begin{bmatrix} e^T(k-1) & r^T(k) & \tilde{y}^T(k) & u_1(k-1) & u_2(k-1) \end{bmatrix}$ as it was observed that the consideration of $v_1(k-1)$ and $v_2(k-1)$ does not have any impact on the performance of the controller. Fig. 5 shows the variations of the side-slip angle β and roll angle ϕ with respect to the trajectories $r_\beta(t)$ and $r_\phi(t)$. As shown Fig. 6, the proposed controller of this note successfully ensures servo tracking while fully complying the actuator limits. Here, it is worth mentioning how a change in the reference r_β at $t = 21$ s has a cross-correlated disturbance effect on the roll angle. This is due to strong cross-couplings in the system dynamics which makes the control difficult.

In order to demonstrate how saturations on the actuators have devastating effects on the closed-loop system's stability, we have also designed an $\mathcal{H}_\infty$ controller for the system using system dynamics (68) and the augmentation (65). For the $\mathcal{H}_\infty$ control algorithm, we employed the design equations given in [44] and obtained an 8th order $\mathcal{H}_\infty$ controller having the minimum achievable closed-loop gain $\gamma_\infty = 0.0711$ which is slightly less than ours. As it follows from Figs. 7 and 8 that saturations on the control signals and their derivatives make the output $\beta(t)$ oscillatory and the roll angle $\phi(t)$ diverging(unstable), although the closed-loop system poles remain in the unit circle.

As a last study, we now consider the case that there is an additive uncertainty on the yaw dynamics in (68) such that

$$\tilde{A}(2,2) = 0.4646 + 0.2\delta_\zeta(k) \tag{70}$$

where $\delta_\zeta(k) \in [-1, 1]$ for all $k \ge 0$. Note that this kind of a time-varying uncertainty can make the open-loop system dynamics unstable for some values of δ_ζ. One can simply represent the uncertain plant dynamics in the form of an LFT (50) with the uncertainty block $\Delta(k) = \delta_\zeta(k)$ and the matrices (71)–(74).

Using the same weighting matrices that we have used in the nominal controller design, the application of the proposed robust output-feedback controller yields a minimum achievable closed-loop gain $\gamma_\infty = 0.0803$ at $\lambda = 0.2507$. Fig. 9 shows the variation of β and ϕ with respect to the reference signals (69) while Fig. 10 demonstrates the variations of control signals for 30 different tests performed on the uncertain system model in which δ_ζ varies randomly. Both studies justify that the proposed robust controller can successfully control the system even under the influential time-varying changes in the system dynamics.

5. Conclusion

We have developed a synthesis methodology for the robust state- and dynamic output feedback controllers for uncertain DT systems. The system we considered is subject to peak-bounded

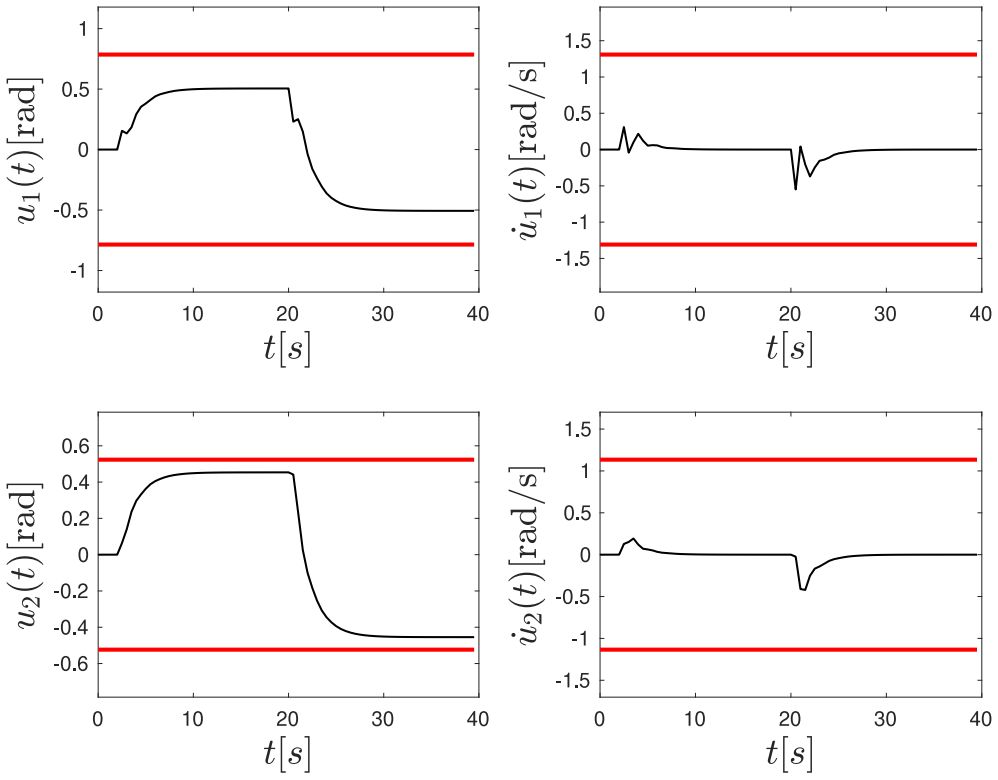

Fig. 6. (Nominal model, Example 2) Time history of the control signals and their rates for the proposed control (black) along with their limit values (red). (For interpretation of the references to colour in this figure legend, the reader is referred to the web version of this article.)

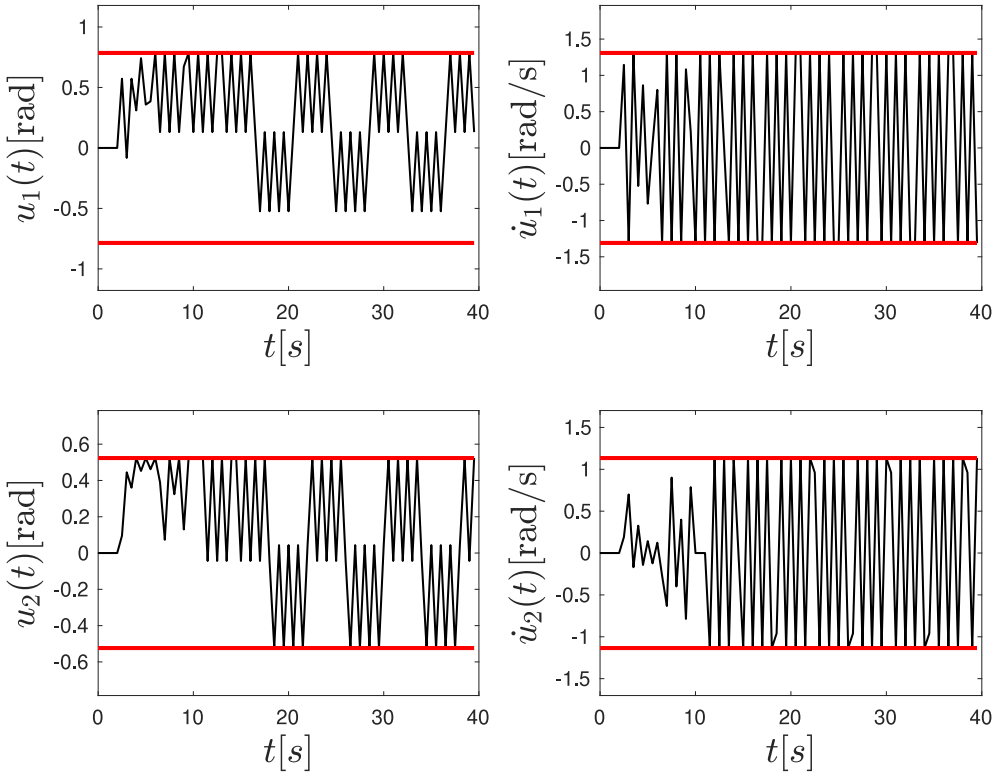

Fig. 7. (Nominal model, Example 2) Variations of the control signals for $\mathcal{H}_\infty$ control (black) and the actuator limits (red). (For interpretation of the references to colour in this figure legend, the reader is referred to the web version of this article.)

disturbances with strict input magnitude and rate bounds. In this note, we have considered extended form representation of the uncertain system to deal with MRBs through peak-to-peak gains of the system as well as the induced ℓ_2 gain from disturbance inputs to the control outputs for the sake of minimising the effects of disturbances, in contrast to what is prevalent in the

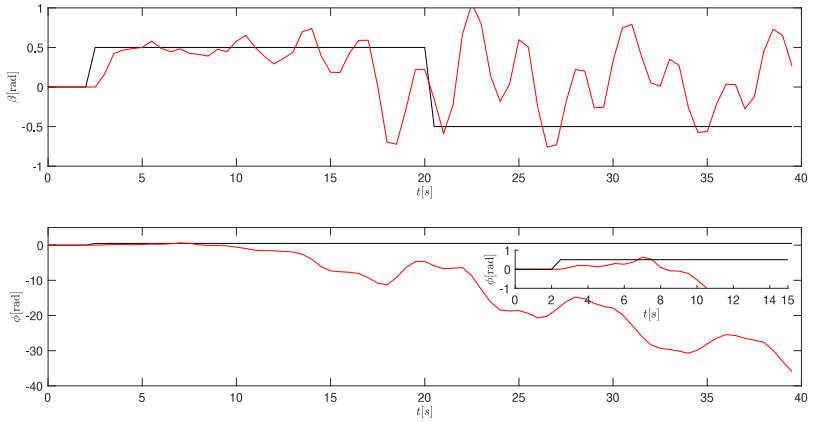

Fig. 8. (Nominal model, Example 2) Variation of the side-slip angle β (top-red) and roll angle ϕ (bottom-red) with respect to reference trajectories r_β (top-black) and r_ϕ (bottom-black) when the system is controlled by discrete-time $\mathcal{H}_\infty$ control without considering of actuator limits. (For interpretation of the references to colour in this figure legend, the reader is referred to the web version of this article.)

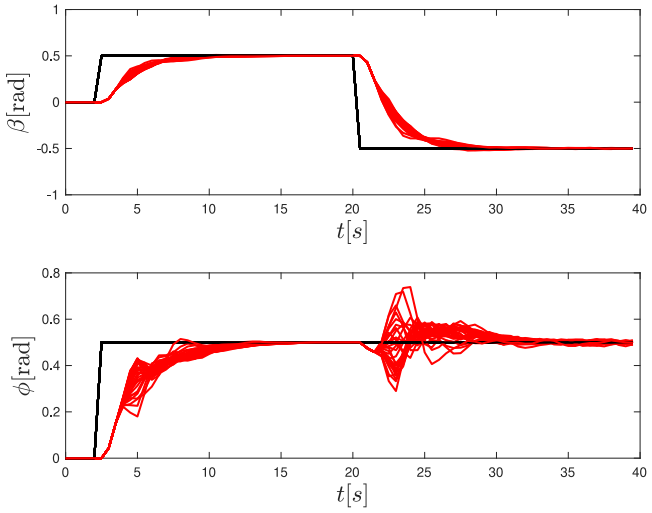

Fig. 9. (Uncertain model, Example 2) Variation of the side-slip angle β (top-red) and roll angle ϕ (bottom-red) with respect to reference trajectories r_β (top-black) and r_ϕ (bottom-black) when the system is controlled by the proposed robust output-feedback control. (For interpretation of the references to colour in this figure legend, the reader is referred to the web version of this article.)

literature. In order to obtain minimal conservatism, we employed extended LMIs during the derivation of the methodology. Later, we have adapted full block S-Procedure to the problem to deal with uncertainties defined by LFTs. We were able to construct a robust controller with low conservatism using the full block S-Procedure, which is applicable not just to systems with affine parameter dependency, but also to any parametric system with rational parameter dependence. At the end of the study, we demonstrated the effectiveness of the proposed schemes through the simulation of two different examples. The simulation results have demonstrated that the proposed method of this paper was very effective and less conservative compared to some recent AW methods provided in the literature. The inevitable conservatism associated with the nature of the peak-to-peak control can be overcome by the application of gain-scheduled techniques to the proposed solution. However, this problem has been left for a future study.

Funding

This research has been funded by the Engineering and Physical Sciences Research Council (EPSRC) of the United Kingdom through the Offshore Robotics for Certification of Assets (ORCA) Hub (EP/R026173/1) under the Partnership Resource Fund project ROBMAN

Declaration of competing interest

The authors declare that they have no known competing financial interests or personal relationships that could have appeared to influence the work reported in this paper.

Appendix

$$\mathcal{A} = \begin{bmatrix} 1 & 0 & 0 & 0 & -1 & 0 & 0 & 0 \\ 0 & 1 & 0 & 0 & 0 & -1 & 0 & 0 \\ 0 & 0 & 0.6740 & 1.3676 & -4.1392 & -0.0463 & -0.1089 & 0.7915 \\ 0 & 0 & 0.0130 & 0.4646 & 1.6521 & 0.0173 & -0.1049 & -0.0431 \\ 0 & 0 & 0.0034 & -0.3894 & 0.4932 & 0.0151 & 0.0592 & 0.0247 \\ 0 & 0 & 0.4141 & 0.2624 & -1.2543 & 0.9917 & 0.0030 & 0.3213 \\ 0 & 0 & 0 & 0 & 0 & 0 & 0.0067 & 0 \\ 0 & 0 & 0 & 0 & 0 & 0 & 0 & 0.0821 \\ 0 & 0 & 0 & 0 & 0 & 0 & 0 & 0 \\ 0 & 0 & 0 & 0 & 0 & 0 & 0 & 0 \\ 0 & 0 & 0 & 0 & 0 & 0 & 0 & 0 \\ 0 & 0 & 0 & 0 & 0 & 0 & 0 & 0 \end{bmatrix}$$

$$\begin{bmatrix} 0 & 0 & 0 & 0 \\ 0 & 0 & 0 & 0 \\ 0.0596 & 3.2129 & 0.0596 & 3.2129 \\ -1.1801 & -0.2088 & -1.1801 & -0.2088 \\ 0.2764 & 0.0509 & 0.2764 & 0.0509 \\ 0.0727 & 0.6627 & 0.0727 & 0.6627 \\ 1.9865 & 0 & 1.9865 & 0 \\ 0 & 1.8358 & 0 & 1.8358 \\ 1 & 0 & 1 & 0 \\ 0 & 1 & 0 & 1 \\ 0 & 0 & 1 & 0 \\ 0 & 0 & 0 & 1 \end{bmatrix} \tag{71}$$

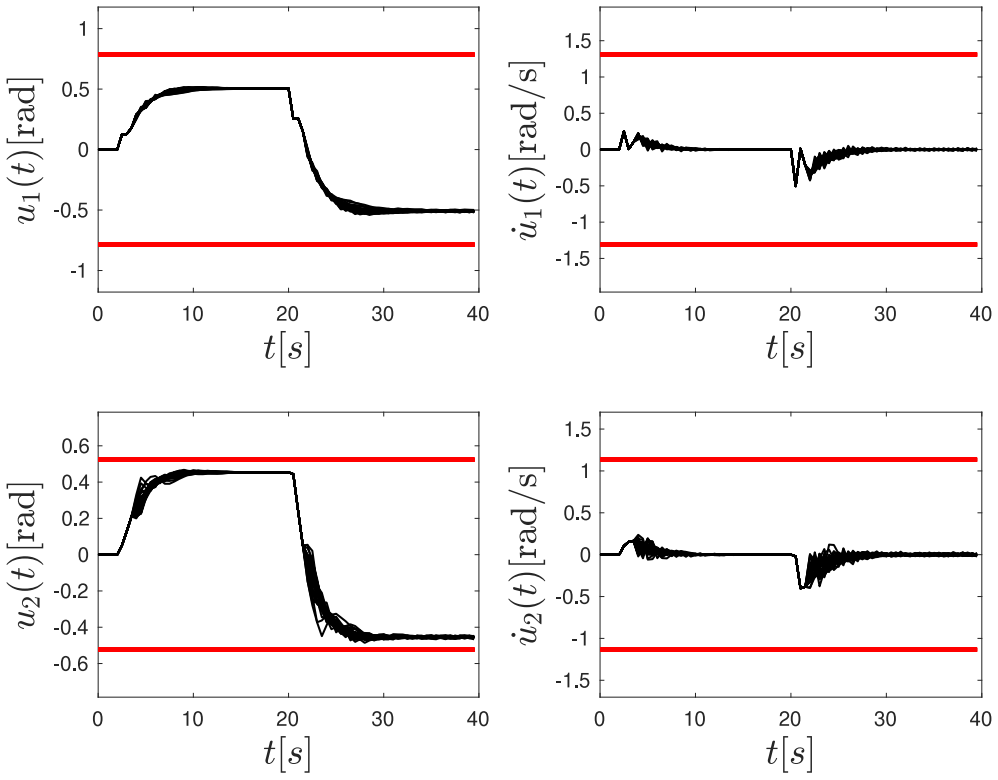

Fig. 10. (Uncertain model, Example 2) Variations of the control signals for the proposed robust output-feedback control (black) and the actuator limits (red). (For interpretation of the references to colour in this figure legend, the reader is referred to the web version of this article.)

$$\left[\mathcal{A}_d \;\middle|\; \mathcal{B}_d \;\middle|\; \mathcal{H}_d\right] = \left[\begin{array}{cccccccccccc|cc|cc} 0 & 0 & 0 & 0.4472 & 0 & 0 & 0 & 0 & 0 & 0 & 0 & 0 & 0 & 0 & 0 & 0 \end{array}\right]. \tag{74}$$

Box II.

$$\left[\mathcal{B} \;\middle|\; \mathcal{H}\right] = \left[\begin{array}{cc|cc} 0 & 0 & 1 & 0 \\ 0 & 0 & 0 & 1 \\ 0.0596 & 3.2129 & 0 & 0 \\ -1.1801 & -0.2088 & 0 & 0 \\ 0.2764 & 0.0509 & 0 & 0 \\ 0.0727 & 0.6627 & 0 & 0 \\ 1.9865 & 0 & 0 & 0 \\ 0 & 1.8358 & 0 & 0 \\ 1 & 0 & 0 & 0 \\ 0 & 1 & 0 & 0 \\ 1 & 0 & 0 & 0 \\ 0 & 1 & 0 & 0 \end{array}\right], \tag{72}$$

$$\begin{aligned} \mathcal{B}_p &= \left[\begin{array}{cccccccccccc} 0 & 0 & 0 & 0.4472 & 0 & 0 & 0 & 0 & 0 & 0 & 0 & 0 \end{array}\right]^T, \\ \mathcal{D}_p &= 0, \end{aligned} \tag{73}$$

and Eq. (74) is given as in Box II.

References

[1] Tarbouriech S, Turner M. Anti-windup design: an overview of some recent advances and open problems. IET Control Theory Appl 2009;3(1):1–19.

[2] Chan P, Catpinar SF, Chang B, Kwatny H, Belcastro CM. Aircraft spiral dive attractors due to actuator saturation. In: 13th IEEE international conference on control automation (ICCA). 2017, p. 1072–7.

[3] Anon. Why the grippen crashed. Aerosp Am 1994;11.

[4] Stein G. Respect the unstable. IEEE Control Syst 2003;23(4):12–25.

[5] Dornheim MA. Report pinpoints factors leading to YF-22 crash. (fighter plane prototype). Aviat Week Space Technol 1992;137(19):53.

[6] Küçükdemiral İB. Robust disturbance rejection for discrete-time systems having magnitude and rate bounded inputs. J Franklin Inst 2020;357(12):8252–76.

[7] Kucukdemiral IB, Yazici H. Robust gain-scheduling H_∞ control of uncertain continuous-time systems having magnitude- and rate-bounded actuators: An application of full block S-procedure. J Franklin Inst 2021;358(16):8226–49.

[8] Wang Y, Murray RM. Bifurcation control of rotating stall with actuator magnitude and rate limits: Part I—model reduction and qualitative dynamics. Automatica 2002;38(4):597–610.

[9] Kucukdemiral IB, Cakici F, Yazici H. A model predictive vertical motion control of a passenger ship. Ocean Eng 2019;186:106100.

[10] Liu Z, He X, Zhao Z, Ahn CK, Li H-X. Vibration control for spatial aerial refueling hoses with bounded actuators. IEEE Trans Ind Electron 2021;68(5):4209–17.

[11] Chen P-C, Shamma JS. Gain-scheduled ℓ1-optimal control for boiler-turbine dynamics with actuator saturation. J Process Control 2004;14(3):263–77.

[12] Stoorvogel A, Saberi A. Editorial (special issue on control problems with constraints). Int J Robust Nonlinear Control 1999;9(10):583–4.

[13] Adamy J, Flemming A. Soft variable-structure controls: a survey. Automatica 2004;40(11):1821–44.

[14] Hu T, Lin Z. Control systems with actuator saturation: analysis and design. Secaucus, NJ, USA: Birkhauser Boston, Inc; 2001.

[15] Hu T, Lin Z, Chen BM. An analysis and design method for linear systems subject to actuator saturation and disturbance. Automatica 2002;38(2):351–9.

[16] Wan Z, Kothare MV. An efficient off-line formulation of robust model predictive control using linear matrix inequalities. Automatica 2003;39(5):837–46.

[17] Hippe P. Windup in control: Its effects and their prevention. Springer Science & Business Media; 2006.
[18] Galeani S, Tarbouriech S, Turner M, Zaccarian L. A tutorial on modern anti-windup design. Eur J Control 2009;15(3-4):418–40.
[19] Kapila V, Grigoriadis K, editors. Actuator saturation control. Marcel Dekker; 2002.
[20] Lu P. Tracking control of nonlinear systems with bounded controls and control rates. Automatica 1997;33(6):1199–202.
[21] Chen P-C. Multi-objective control of nonlinear boiler-turbine dynamics with actuator magnitude and rate constraints. ISA Trans 2013;52(1):115–28.
[22] Oliveira LAL, Barbosa MVC, Silva LFP, Leite VJS. Exponential stabilization of LPV systems under magnitude and rate saturating actuators. IEEE Control Syst Lett 2022;6:1418–23.
[23] Tohidi SS, Yildiz Y. Handling actuator magnitude and rate saturation in uncertain over-actuated systems: a modified projection algorithm approach. Int J Control 2020;In press:1–14.
[24] Alazki H, Poznyak A. Robust output stabilization for a class of nonlinear uncertain stochastic systems under multiplicative and additive noises: The attractive ellipsoid method. J Ind Manage Optim 2016;12(1):169–86.
[25] Azhmyakov V. On the geometric aspects of the invariant ellipsoid method: Application to the robust control design. In: 50th IEEE conference on decision and control and European control conference. 2011, p. 1353–8.
[26] Azhmyakov V, Poznyak A, Gonzalez O. On the robust control design for a class of nonlinearly affine control systems: The attractive ellipsoid approach. J Ind Manage Optim 2013;9(3):579–93.
[27] Gonzalez O, Poznyak A, Azhmyakov V. On the robust control design for a class of nonlinear affine control systems: the invariant ellipsoid approach. In: 2009 6th international conference on electrical engineering, computing science and automatic control. 2009, p. 1–6.
[28] Poznyak A, Polyakov A, Azhmyakov V. Attractive ellipsoids in robust control. Springer; 2014.
[29] Poznyak A, Azhmyakov V, Mera M. Practical output feedback stabilisation for a class of continuous-time dynamic systems under sample-data outputs. Int J Control 2011;84(8):1408–16.
[30] Baiomy N, Kikuuwe R. An amplitude- and rate-saturated controller for linear plants. Asian J Control 2020;22(1):77–91.
[31] Baiomy N, Kikuuwe R. An amplitude- and rate-saturated collective pitch controller for wind turbine systems. Renew Energy 2020;158:400–9.
[32] Wang S, Gao Y, Liu J, Wu L. Saturated sliding mode control with limited magnitude and rate. IET Control Theory Appl 2018;12(8):1075–85.
[33] Mayne DQ. Model predictive control: Recent developments and future promise. Automatica 2014;50(12):2967–86.
[34] Bender FA, Gomes da Silva Jr JM. Output feedback controller design for systems with amplitude and rate control constraints. Asian J Control 2012;14(4):1113–7.
[35] Galeani S, Onori S, Teel A, Zaccarian L. A magnitude and rate saturation model and its use in the solution of a static anti-windup problem. Syst Control Lett 2008;57(1):1–9.
[36] Reineh MS, Kia SS, Jabbari F. New anti-windup structure for magnitude and rate limited inputs and peak-bounded disturbances. Automatica 2018;97:301–5.
[37] Bateman A, Lin Z. An analysis and design method for linear systems under nested saturation. Syst Control Lett 2003;48(1):41–52.
[38] Palmeira AHK, Gomes Da Silva JM, Tarbouriech S, Ghiggi IMF. Sampled data control under magnitude and rate saturating actuators. Int J Robust Nonlinear Control 2016;26(15):3232–52.
[39] Tarbouriech S, Prieur C, Da Silva J. Stability analysis and stabilization of systems presenting nested saturations. IEEE Trans Autom Control 2006;51(8):1364–71.
[40] Zhou B. Analysis and design of discrete-time linear systems with nested actuator saturations. Syst Control Lett 2013;62(10):871–9.
[41] Köse IE, Jabbari F. Rate and magnitude-bounded actuators: Scheduled state feedback design. In: 15th IFAC world congress. IFAC Proceedings Volumes; 2002, p. 73–8.
[42] Jabbari F, Köse IE. Rate and magnitude-bounded actuators: scheduled output feedback design. Int J Robust Nonlinear Control 2004;14(13-14):1169–84.
[43] Chellaboina VS, Haddad WM, Oh JH. Fixed-order dynamic compensation for linear systems with actuator amplitude and rate saturation constraints. Int J Control 2000;73(12):1087–103.
[44] Oliveira MCD, Geromel JC, Bernussou J. Extended H_2 and H_∞ characterizations and controller parametrizations for discrete-time systems. Int J Control 2002;75(9):666–79.
[45] Scherer CW. A full block s-procedure with applications. In: 36th IEEE conference on decision and control. 3, 1997, p. 2602–7.
[46] Wang L. A tutorial on model predictive control: Using a linear velocity-form model. Dev Chem Eng Miner Process 2004;12(5):573–614.
[47] Shaked U, Yaesh I. Robust servo synthesis by minimization of induced ℓ_2 and ℓ_∞ norms. In: 2007 IEEE international symposium on industrial electronics. 2007, p. 24–9.
[48] Boyd S, El Ghaoui L, Feron E, Balakrishnan V. Linear matrix inequalities in system and control theory. Studies in applied mathematics, vol. 15, Philadelphia, PA: SIAM; 1994.
[49] Scherer C, Weiland S. Lecture notes: Linear matrix inequalities in control. Delft, The Netherlands: Dutch Institute for Systems and Control; 2015.
[50] Gupta A, Koroglu H, Falcone P. Computation of low-complexity control-invariant sets for systems with uncertain parameter dependence. Automatica 2019;101:330–7.
[51] Parrilo PA. Structured semidefinite programs and semialgebraic geometry methods in robustness and optimization (PhD thesis), California Institute of Technology; 2000.
[52] Scherer C. LMI relaxations in robust control. Eur J Control 2006;12(1):3–29.
[53] Koroglu H, Scherer C. Robust stability analysis against perturbations of smoothly time-varying parameters. In: 45th IEEE conference on decision and control. 2006, p. 2895–900.
[54] Lofberg J. YALMIP : A toolbox for modeling and optimization in MATLAB. In: 2004 IEEE international conference on robotics and automation. 2004, p. 284–9.
[55] Ochi Y, Kanai K. Pole placement in optimal regulator by continuous pole-shifting. J Guid Control Dyn 1995;18(6):1253–8.